INVESTIGATING THE OPTICAL PROPERTIES OF ZINC SULPHIDE THIN FILMS DEPOSITED FROM CHEMICAL ACIDIC BATHS

BY

ANTHONY OWUSU ANSAH, BSc.Physics (Hons.)

A Thesis submitted to the Department of Physics, Kwame Nkrumah University of Science and Technology, in partial fulfillment of the requirement for the degree of

MASTER OF SCIENCE (SOLID STATE PHYSICS)

College of Science

APRIL, 2012

DECLARATION

I hereby declare that this submission is my own work towards the M.Sc. and that, to the best of my knowledge, it contains no material previously published by any person nor material which has been accepted for the award of any other degree of the University, except where due acknowledgment has been made in the text.

Anthony Owusu Ansah

…… …… ……..

Student Signature Date

Certify by;

K. Ampong

…… …… ……..

Supervisor Signature Date

Certify by;

Prof. S. K. Danuor

…… …… ……..

Head of Department Signature Date

ABSTRACT

A well adherent thin film of zinc sulphide (ZnS) has been deposited on silica glass substrates from acidic baths containing zinc chloride, thioacetamide and urea. Films of different thickness (684nm, 572nm, 523nm, and 271nm) were obtained. SEM micrograph of the as-deposited ZnS thin film, show the film to be uniform, dense, homogenous, and composed of largely irregular shaped grains of diameter in the range of 300 – 500 nm. These large grains are comprised of smaller spherical grains of 100 – 200 nm diameter. EDAX results are consistent with the formation of thin films of ZnS deposited on silica glass substrates. A UV mini Schimazu UV – VIS Spectrophotometer was used to determine the optical absorbance of the films as a function of wavelength at room temperature over the wavelength range 200 – 800 nm. The samples were then thermally annealed for one hour, at temperatures of 300°C, 400°C and 500°C, after which the absorbance of the films were again recorded. The absorbance of the films decreased with increasing annealing temperatures indicating an increase in transmittance with increasing annealing temperatures. The band gap values obtained varied between 3.64 eV and 3.97 eV, for as deposited films and increased between 3.98 eV and 4.00 eV after annealing. The increase in band gap with annealing temperature might be attributed to the improvement in crystallinity in the films. The high transmittance of the films together with their large band gap makes them good materials for application as a window layer for solar cells.

CONTENTS Page

CHAPTER FOUR

CHAPTER FIVE

CHAPTER SIX

LIST OF TABLES

LIST OF FIGURES

ABBREVIATIONS AND ACRONYMS

A	Absorbance
α	Absorption coefficient
BDH	British Drug House
CBD	Chemical Bath Deposition
CdO	Cadmium Oxide
CdS	Cadmium Sulfide
CGS	Copper-Gallium-Selenide
CIS	Copper-Indium-Selenide
CIGS	Copper-Indium-Gallium-Selenide
CVD	Chemical Vapor Deposition
DOS	Density of States
ED	Electron Diffraction
EDAX	Energy Dispersive X-Ray analysis
h	Planck constant
HP	Hewlett-Packard
IR	Infrared
k	Wave vector, Extinction coefficient

$\boldsymbol{\lambda}$	Wavelength
M	Molar concentration
MBE	Molecular Beam Epitaxy
P	Film Packing Factor
P(r)	Radial distribution function
ρ	Resistivity
SEM	Scanning Electron Microscopy
T	Transmittance
TEA	Triethanolamine
$\boldsymbol{\tau_h}$	Heating time
$\boldsymbol{\tau_c}$	Cooling time
UV	Ultraviolet
v	Photon frequency
VIS	Visible Spectrum
x, y	Compositional parameters/an integer number in polyacetylene
XRD	X-Ray Diffraction
ZnS	Zinc Sulfide

ACKNOWLEDGMENTS

My deepest gratitude goes to almighty God who endowed me with health, grace, wisdom, patience and direction to bring this project to completion.

I fully acknowledge my indebtedness to Mr. K. Ampong, Professors F. Boakye, Professors R. K. Nkum, Mr. I. K. Nkrumah and Dr. Michael K. E. Donkor all of the Physics department KNUST, for their direction, pieces of advice and monitoring during the project.

I finally express my sincere thanks to my wife, Beatrice Amponsah, my mother and siblings for their financial support, and passionate prayers throughout the entire period.

CHAPTER ONE

1. INTRODUCTION

Semiconducting materials play an indispensable role in contemporary electronics. In the early days of radio and television, transmitting and receiving equipment relied on vacuum tubes, but these have been almost completely replaced in the last four decades by semiconducting materials, including transistors, diodes, integrated circuits and other solid-state devices (Young and Freedman, 2008). Such devices have found wide application because of their compactness, reliability, power efficiency, and low cost. As discrete components, they have found use in power devices, optical sensors, and light emitters, including solid-state lasers. They have a wide range of current- and voltage-handling capabilities and, more important, lend themselves to integration into complex but readily manufacturable microelectronic circuits. They are, and will be in the foreseeable future, the key elements for the majority of electronic systems, serving communications, signal processing, computing, and control applications in both the consumer and industrial markets (Encyclopedia Britannica, 2010).

The study of semiconducting materials began in the early 19th century. The elemental semiconducting materials are those composed of single species of atoms, such as silicon (Si), germanium (Ge), and tin (Sn) in group IV and selenium (Se) and tellurium (Te) in group VI of the periodic table. During the early 1950s germanium was the major semiconductor material. However, it proved unsuitable for many applications, because devices made of the material exhibited high leakage currents at only moderately elevated temperatures. Since the early 1960s silicon has become by far the most widely used

semiconductor, virtually supplanting germanium as a material for device fabrication. The main reasons for this are twofold: (1) silicon devices exhibit much lower leakage currents, and (2) silicon dioxide (SiO_2), which is a high-quality insulator, is easy to incorporate as part of a silicon-based device. Thus, silicon technology has become very advanced and invasive, with silicon devices constituting more than 95 percent of all semiconductor products sold worldwide.

The potential applications of chalcogenide based materials in electronic and optoelectronic devices are vast, but has received little attention until recently due to the cheap and wide availability of silicon based alternatives (Tan, 2006). Chalcogenide II-VI, compound semiconductors, such as zinc sulphide (ZnS) has generated a lot of interest among scientists because of its extensive use in the fabrication of solid state devices such as solar cells, thin film transistors and electroluminescent displays.

ZnS is an important II-VI group semiconductor with a large direct band gap of 3.5–3.7 eV in the UV range (Vipin *et al.*, 2008). Zinc sulphide is a white to yellow-colored powder or crystal with molecular mass of 97.474 $gmol^{-1}$ and density of 4.090 gcm^{-3}. It is typically encountered in the more stable cubic form, known also as zinc blende or sphalerite. The hexagonal form is also known both as a synthetic material and as the mineral wurtzite. Both sphalerite and wurtzite are intrinsic, wide-band gap semiconductors. The cubic form has a band gap of 3.54 eV at 300 K whereas the hexagonal form has a band gap of 3.91 eV (Wells, 1984). ZnS has a melting point (phase transition) of 1020 ^oC. The cubic form is stable at room temperature, while the less dense hexagonal form (wurtzite) is stable above 1020 ^oC at atmospheric pressure (Gilbert *et al.,* 2002). Figure 1.1 shows each crystal structure.

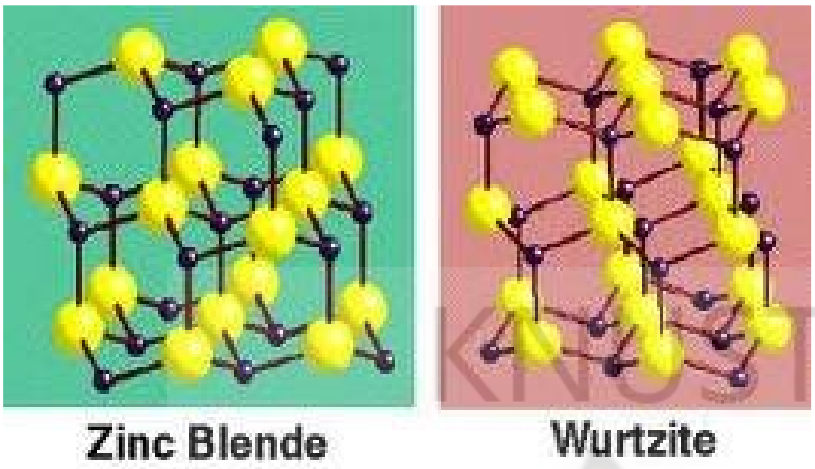

Figure 1.1 The sphalerite or zinc blende and the wurtzite crystal structure of ZnS (chem.ox.ac.uk).

The sphalerite structure can be derived from a cubic close packing of ions, while the wurtzite structure is derived from a hexagonal close packing scheme. This situation is not that simple however, because the difference in energy of the two structures is small (Boggess *et al.,* 2004). Arterton *et al.*, (1992) reported that electroluminescent material must contain both sphalerite and wurtzite phases. The wurtzite type structure predominates when the bonding is primarily ionic whereas the more covalent systems favor the sphalerite form. The nature of the end product is usually dependent on heat treatment temperature, cooling profile, and cooling atmosphere. One phase can be more suitable than another in certain applications. The cubic phase of ZnS is not grown as easily as the hexagonal phase, thus making the hexagonal phase more appealing for electroluminescence device applications (Bellotti *et al.,* 1998). ZnS was used by Ernest Rutherford and others in the early years of nuclear physics as a scintillation detector,

because it emits light on excitation by X-rays or electron beam, making it useful for X-ray screens and cathode ray tubes. It also exhibits phosphorescence due to impurities on illumination with blue or ultraviolet light (Greenwood *et al.*, 1984).

ZnS thin films have been found valuable in various devices. The application of ZnS thin films which cover a wide area of interest are.

- Antireflection coating for the solar cell (Blos *et al*., 1988)
- Environmental friendly buffer layer as compared to CdS layer in CIS based thin film solar cell (Katsumi, 1995)
- Wide band gap material for electroluminescent and optoelectronic devices (Tong *et al.*, 1996).
- Photosynthetic coating (Ndukwe *et al.*, 1996).
- Blue light emitting laser diodes (Hasse *et al.,* 1991).
- As α- particle detector (Kashani, 1996).

In thin film solar cells based on $CuGaIn(S, Se)_2$ absorbers, a CdS (Cadmium Sulphide) buffer layer is generally required in order to obtain high conversion efficiency. However, there are toxic hazards with respect to the production and use of the CdS layer. Therefore research in developing Cadmium (Cd) free buffer layers has been encouraged. This has lead to the investigation of ZnS as a buffer layer in ZnO / ZnS / $CuInS_2$ devices (Borges *et al*., 1992). ZnS has a wider energy band gap than CdS, which results in the transmission of more high-energy photons to the junction, and to the enhancement of the blue response of the photovoltaic cells.

Zinc sulphide (ZnS) thin films with a wide direct band gap and n-type conductivity are promising for optoelectronic device applications, such as electroluminescent devices and photovoltaic cells. In optoelectronics, it can be used as light emitting diode in the blue to ultraviolet spectral region due to its wide band gap of 3.7 eV at room temperature (Yamaga *et al.*, 1998). In the area of optics, ZnS can be used as a reflector and dielectric filter because of its high refractive index (2.35) and high transmittance in the visible range, respectively (Ruffer *et al.*, 1998; Ledgar,1979).

In recent times, the study of semiconductors in the bulk has been replaced with that of thin films. Thin film technique is one of the most fully-fledged technologies that greatly contribute to developing the study of semiconductors by giving a clear indication of their chemical and physical properties. Thin films have mechanical, electrical, magnetic and optical properties which may differ from those of the bulk material and are used commonly in the form of a deposit on a suitable substrate. Presently, rapidly changing needs for thin film materials and devices are creating new opportunities for the development of new processes, materials and technologies.

There exists a huge variety of thin film deposition processes and technologies which originate from purely physical or purely chemical processes. These include vacuum evaporation, spray pyrolysis, sputtering molecular beam epitaxy, vapour phase epitaxy, chemical vapour deposition, solution growth, screen printing and electrophoresis. Despite the existence of these large variety of deposition techniques, searching for the most reliable and economic deposition technique has always been the main goal. Of all the techniques mentioned chemical bath deposition is currently attracting a great deal of

attention as the techniques is relatively simple and cost effective, has minimum material wastage, does not need sophisticated instrument and vacuum, and can be applied in large area deposition at low temperature. This method uses a controlled chemical reaction to deposit a thin film. In the typical experimental approach, the substrates are immersed in solution containing the Chalcogenide source, metal ion, and complexing agent (Kassim *et al.,* 2009).

To make semiconducting thin films useful in any given applications, it is very important to investigate their optical properties. Optical properties are directly related to structural and electronic properties of solids, and hence very important in device applications. A detailed knowledge of optical properties can provide a huge amount of information about their structure, optoelectronic behavior, transport of charged carriers, etc. (Singh and Shimakawa, 2003). These are important parameters for scientists and technocrats to decide its end use.

This thesis is primarily concerned with the investigation of the optical properties of zinc sulphide thin films deposited from chemical acidic baths.

1.1 OBJECTIVES OF THE PROJECT

The research presented in this thesis was motivated by the following objectives:

- To deposit zinc sulphide thin films from chemical acidic baths containing zinc chloride, thioacetamide and urea.

- To investigate the optical properties, morphology, structure and elemental composition of the thin films.
- To analyze the effect of thermal annealing on the optical band gap of the thin films.

1.2 JUSTIFICATION OF THE PROJECT

Efforts have been made currently for finding new materials for low cost energy conversion. Among the materials of recent research interest are CdS, CdSe, ZnSe, ZnS, etc., which fall in the group of II-VI family of compounds (Zainel et. Al., 1996), due to their photo- and electro- luminescence properties and promising applications in optoelectronics. The recent surge of activity in wide band gap materials like ZnS has arisen from the need for electronic devices operating at high power levels and high temperatures. ZnS is an attractive material due to its properties like direct band gap and transparency over a wide range of the visible spectrum.

1.2.1 Reasons for choosing the Chemical Bath Deposition technique

There is considerable interest in the deposition of compound semiconductors by methods which involve relatively low capital expense and are technically undemanding on the experimentalist. One process to meet these criteria is Chemical Bath Deposition (CBD). Such processing methods are particularly appropriate for the production of devices for which large areas substrates and low cost are essential such as solar cells.

1.2.2 Why Chemical Acidic Baths

Typical CBD processes for sulphides employ an alkaline medium containing the chalcogenide source, the metal ion and added base. A chelating agent is used to limit the hydrolysis of the metal ion and impart some stability to the bath, otherwise undergo rapid hydrolysis and precipitation. The technique under these conditions relies on the slow release of S^{2-} ions into an alkaline solution in which the free metal ion is buffered at a low concentration (Boyle et al, 1999).

However, the deposition of ZnS films appears to be remarkably difficult to achieve in alkaline solutions due to the stability of the hydroxyl species (Boyle et al, 1999). In particular it is evident that there is a much wider range of conditions in which the concurrent deposition of zinc sulphide and oxide can occur (O'Brien and McAleese, 1998). Many of the films reported as ZnS which have not been rigorously characterized are probably at best heavily contaminated with zinc oxide or hydroxide (O'Brien and McAleese, 1998). For this reason, hydroxide formation needs to be minimized in order to form quality CBD zinc sulphide thin films (Edelson, 2007). This has led to development of a more favourable medium for formation of ZnS thin films.

Lincot et al, (1992) developed the deposition of ZnS from acidic solutions in which urea hydrolysis is used to control the pH and produced among the best ZnS films reported to date. These factors have informed our choice of using an acidic medium for the deposition of ZnS instead of an alkaline medium associated with the conventional CBD process.

1.2.3 Why investigate the Optical properties, Structure, and Morphology of the thin film

Several authors have reported the deposition of zinc sulphide thin films from acidic solutions containing various chemicals of varying concentrations and under different deposition conditions. However, semiconductor devices based on thin films strongly depend on the structural and optical properties of films obtained from various experimental conditions such as temperature, pH of the solution, stirring and rate of deposition. These conditions can cause the structural and optical properties of films as well as qualities, such as distribution of states within the film to differ, and hence the need to investigate these properties for any preparatory method used. Also, being able to 'tune' the optical properties through thermal annealing can result in materials for specific applications.

1.3 STRUCTURE OF THESIS

The thesis is organized into five chapters. The first chapter gives an introduction to the impact of semiconductor research over the years, some physical properties of semiconductors and why the interest in compound semiconductor materials such as ZnS. The chapter also looks at the structure of ZnS and states the specific research objectives and finally describes how the thesis is structured.

The second chapter deals with review of literature on ZnS. Emphasis is placed on the optical and transport properties of ZnS deposited with different methods under different conditions and the effects of thermal annealing on the optical properties. The third chapter treats the relevant theory.

Methodology and materials used in carrying out this research are presented in the fourth chapter, whiles the fifth chapter deals with results in graphical format and in-depth discussion of results. In the sixth chapter conclusions and recommendations are made. Lastly, references cited in this thesis and appendices are presented.

CHAPTER TWO

2. LITERATURE REVIEW

The solids known as semiconductors have been the subject of very extensive research over recent decades, not simply because of their intrinsic interest but also because of ever more numerous and powerful applications: rectifiers, transistors, photoelectric cells, magnetometers, solar cells, reprography, lasers, and so forth.

Starting with the development of the transistor by John Bardeen, Walter Brattain and William Shockley at Bell Telephone Laboratories in 1947, the technology of semiconductors has exploded. With the creation of integrated circuits and chips, semiconductor devices have penetrated into large parts of our lives. The modern desktop or laptop computer would be unthinkable without microelectronic semiconductor devices, and so would a myriad of other devices (Petterson and Bailey, 2005).

In recent times, the study of semiconductors in the bulk have been replaced with that of thin films. Involvement with thin films dates to the metal ages of antiquity. As a modern science, thin films have been prepared ever since vacuum systems first became available, but deposition as a means of producing films for device purposes is a development of the past 40 years. Thin metallic film coatings on glass or plastic were among the first to be exploited for optical purposes, ranging from mirrors to sunglasses, and this still continues as a major, typically high vacuum, high throughput business.

Semiconductor thin film technology has attracted much attention, because of its matchless size dependent properties and applications in the optoelectronics devices, solar cells, sensors and laser materials. As thin film deposition processes have developed very

rapidly over the past 25 years, particularly in the context of semiconductor devices, processes have become highly specialized (Ohring, 1992; Venables, 2003).

Sulphide thin films such as zinc sulphide (ZnS) has generated a lot of interest among scientists because of its extensive use in the fabrication of solid state devices. There is a diverse range of applications of thin films of this semiconductor and this is reflected in the large amount of literature available on its properties reported by various authors using different deposition techniques.

In 2008, Ilenikena successfully produced semiconductor thin films of copper sulphide (CuS) and zinc sulphide (ZnS) on glass microscope slides at 320 K and pH values of 7, 9, 10, 11 and 12 using improved chemical bath deposition method. The results show that pH increases with the optical and solid-state properties (such as transmittance, energy gap, refractive index, absorption coefficient, dielectric constant, thickness and so on) of the films.

The results obtained by Nadeem and Ahmed (2000) and Ndukwe (1996) on the optical absorbance of ZnS thin films for wavelengths in the infrared (up to 1000 nm) and visible spectrum showed that ZnS is practically non-absorbing in these regions. Similar behavior was observed by Hammer (1943) in the visible region. ZnS films deposited on the glass substrate at room temperature have shown an enhanced absorption in the neighborhood of $\lambda = 330$ nm (Huldt and Staflin, 1959, Gonellian, 1996) and 360 nm (Nadeem and Ahmed, 2000) and were expected to have a fine grained structure. The absorption peak shifts towards longer wavelength with increasing thickness. Ndukwe (1996) also observed that

some ZnS films have high absorbance (~ 0.56) in the near infrared and low absorbance (~ 0.01 – 0.1) in the ultraviolet and visible region.

In 1951, Rood reported that rapidly evaporated ZnS films had a high optical absorption and claimed that the deposition rate for producing good quality films should be about 0.16 nms^{-1}. Polster (1952) found that the rapidly deposited ZnS films (1.6 nms^{-1}) had considerable light absorption, but the films formed at about 0.5 nms^{-1} had negligible absorption. He claimed that large ZnS crystals are formed at high deposition rates and this increased the amount of light lost by scattering within the film. The result was opposite to the general experience because the grain size of most substances falls as the rate of deposition increases. Decomposition of evaporant may explain the greater light absorption of rapidly deposited ZnS thin films. At high rates of evaporation corresponding to high source temperature, free zinc atoms may be trapped in the condensed film. At low evaporation rates decomposition may be less and there is also ample opportunity for free zinc atoms to oxidize either at the condensing surface or in the region of the source. Zinc oxide has a refractive index comparable to that of ZnS and if present in the deposit would not be easily detected.

ZnS films prepared by Nadeem and Ahmed (2000) using resistive heating technique had high transmittance (60–99 %) in the visible and near infrared region. ZnS thin films coated on Ge (Yamanishi *et al.,* 1985) using ionized cluster beam (ICB) method were found to have a transmittance of 96 %. So they are useful as an antireflection coating for the optical transmission window. Yamaguchi *et al*., (1996) deposited the (Cd, Zn)S thin films on Corning 7059 glass substrate using chemical bath deposition (CBD) technique for photovoltaic devices. Thin films with zero concentration of Cd demonstrated more

than 70 % transmittance at Wavelengths longer than 600 nm. ZnS films grown by Ndukwe (1996) had high transmittance (~ 64–98 %) in the visible and near infrared regions. He also observed that some of the films had low transmittance (~ 30–37 %) in near infrared region and high transmittance (~ 78–98 %) in the visible and ultraviolet region. The transmittance of ZnS films grown on polyester foils (Lindroos *et al*. 1997) using successive ionic layer adsorption and reaction method was more than 60 % above 400 nm.

Hass *et al*., (1982) have reported that ZnS films deposited at high rates and low pressures are found to exhibit bulk values of refractive index when evaporated at room temperature. Hammer (1943) observed that the refractive index for thinner ZnS films were lower than those for thicker films. The presence of voids, more marked in the thinnest films gave rise to the mean refractive index below that of bulk material. Nadeem and Ahmed (2000), Ndukwe (1996) and Polster (1952) found that refractive index vary with the wavelength of the incident light, where as for the films analyzed by Nesmelov *et al.,* (1984) refractive index seems to be dependent on the growth rate. The refractive index of bulk ZnS is 2.4 (Hu and White 1983).

Lindroos *et al.,* (1994) grew ZnS thin films using successive layer adsorption and reaction (SILAR) technique on soda lime glass, ITO - and Al_2O_3 - covered glass and Si substrate and found that the films were inhomogeneous and of poor quality. According to them, the XRD analysis showed that their ZnS films were polycrystalline and presumably cubic. The refractive indices varied from 2.07 to 2.19 on glass grown ZnS films and from 2.15-2.30 on ITO – covered glass.

In 1960, W. Crawford Dunlap, Jr. estimated the band gap ZnS by means of photoconductivity and optical process and came out with 3.67 eV and 3.58 eV respectively. He attributed the difference in energy gap to experimental error or to a temperature difference in band gap, amounting to $3x10^{-4}$ $eV.K^{-1}$.

The band gap of ZnS thin films found by various scientists using different techniques has been summarized in Table 1 (see appendix A).

2.1 Principles of Chemical Bath Deposition (CBD)

As mentioned in chapter one, CBD method is most commonly used because it is a very simple, cost effective and economically reproducible technique that can be applied in large area deposition at low temperature. Chemical bath deposition is used to deposit thin films of a wide-range of materials (Nair *et al*., 1998 and Savadogo, 1998). The deposition mechanism is largely the same for all such materials. A soluble salt of the required metal is dissolved in an aqueous solution, to release cations. The non-metallic element is provided by a suitable source compound, which decomposes in the presence of hydroxide ions, releasing the anions. The anions and cations then react to form the compound (Johnston et al, 2002). The source materials used in this work were zinc chloride ($ZnCl_2$) and thioacetamide (C_2H_5NS).

This technique is based on the controlled release of metal ion (M^{2+}) and sulphide (S^{2-}) or selenide (Se^{2-}) ions in an aqueous bath in which the substrates are immersed. In this process, release of metal ion (M^{2+}) is controlled by using a suitable complexing agent. The deposition begins with nucleation phase followed by growth phase in which the

thickness of film increases with duration up to the terminal phase where film depletion into constituent ions occurs after a certain time.

Typical CBD processes for sulphides employ an alkaline medium containing the chalcogenide source, the metal ion and added base. A chelating agent is used to limit the hydrolysis of the metal ion and impart some stability to the bath, which would otherwise undergo rapid hydrolysis and precipitation. The technique under these conditions relies on the slow release of ions into an alkaline solution in which the free metal ion is buffered at a low concentration. There are a few reports of the CBD of the binary ZnS (Padam et al, 1988; Chopra et al, 1982); the most convincing studies demonstrate that the production of good quality thin films is very difficult by conventional chemical bath systems (Al-Kuhami et al, 2000) due to the stability of hydroxyl species. Unlike, cadmium and lead chalcogenides in which the formation of hydroxide species in solution is an important factor for the formation of high quality films, ZnS is not favoured with the hydroxide formation. The relatively small difference in the solubility products of zinc sulphide and zinc hydroxide leads to possible competition between the formation of sulphide and hydroxide in alkaline solutions, with the presence of significant quantities of oxides or hydroxides observed in CBD zinc sulphide films (O'Brien et al,1998 and Lincot et al,1995). For this reason, hydroxide formation needs to be minimized in order to form quality CBD zinc sulphide thin films (Edelson, 2007). This has led to development of a more favourable medium for formation of ZnS thin films.

Lincot et al, (1992) developed the deposition of ZnS from acidic solutions in which urea hydrolysis is used to control the pH and produced among the best ZnS films reported to date.

2.2 ANNEALING

Annealing is heat treatment of materials at elevated temperatures aimed at investigating or improving their properties. Material annealing can lead to phase transitions, recrystallization, polygonization, homogenization, relaxation of internal stresses, removal of after effects of cold plastic deformation (strain hardening), annihilation and rearrangement of defects and so on. The results of annealing depend significantly on its kinetics: the rate of heating and cooling and the time of exposure at a given temperature.

2.2.1. IRRADIATION ANNEALING

This is the annealing of defects in a crystal stimulated by nuclear radiations. Both impurity atoms and other defects formed prior to irradiation, as well as radiation-induced defects take part in the process. When radiation doses are large, annealing lowers the rate of accumulation of the defects, particularly if the intensities are high enough. Irradiation annealing mechanisms are related to the processes of radiation-induced diffusion of defects, to atomic restructuring triggered by collisions of external particles with crystal atoms and also the small dose effect (Poole, 2004).

2.2.2. RECRYSTALLIZATION ANNEALING

Heating a solid to a temperature that provides full recrystallization within a given time period. Recrystallization annealing is used to lower the dislocation density, to change texture, to form a polycrystal structure and thereby to bring the physical and chemical properties of a solid to a level characteristic of an unhardened annealed state. Conditions for this annealing of deformed materials are chosen using recrystallization diagrams

which provide the dependences of the temperatures for the beginning and end of the initial recrystallization on the degree of strain for a given processing duration.

2.2.3. PULSED ANNEALING OF SEMICONDUCTORS

This is a high temperature treatment of semiconductor specimens which is characterized by sharp fronts of heating τ_h and cooling τ_c, in practice without holding the temperature at the maximum value. Values of τ_h and τ_c vary over a wide range. As a rule, they are set by the conditions of conserving the bulk properties, without noticeable diffusion of impurities, and this provides the possibility of fusing surface layers while conserving the crystal structure of the bulk. The process duration is from 10^{-12} s to several seconds. For pulses shorter than a few microseconds the most efficient results are achieved with exciting pulse energies sufficient for melting the surface layer. For longer pulses the target heating is almost uniform due to thermal conductivity. Particularly important results were obtained by combining pulsed annealing with ion implantation of impurities. The nonequilibrium introduction of impurities together with nonequilibrium annealing is the most efficient technique for obtaining highly doped, structurally perfect semiconducting layers. The pulsed annealing method is widely used for the restoration of a crystal structure disturbed during ion bombardment (Poole, 2004).

CHAPTER THREE

3. THEORETICAL BACKGROUND

3.0. CLASSIFICATION OF SOLIDS

There are diverse ways of classifying solids, but perhaps the most useful division is into crystalline, polycrystalline and amorphous. Each type is characterized by the size of an ordered region within the material. An ordered region is spatial volume in which atoms or molecules have a regular geometric arrangement or periodicity. Figure 3.1 shows the three structural orders (Neamen, 2003). It should be noted that the majority of semiconductors used in electronic applications are crystalline materials, although some polycrystalline and amorphous semiconductors have found a wide range of applications in various electronic devices, (Yacobi, 2004).

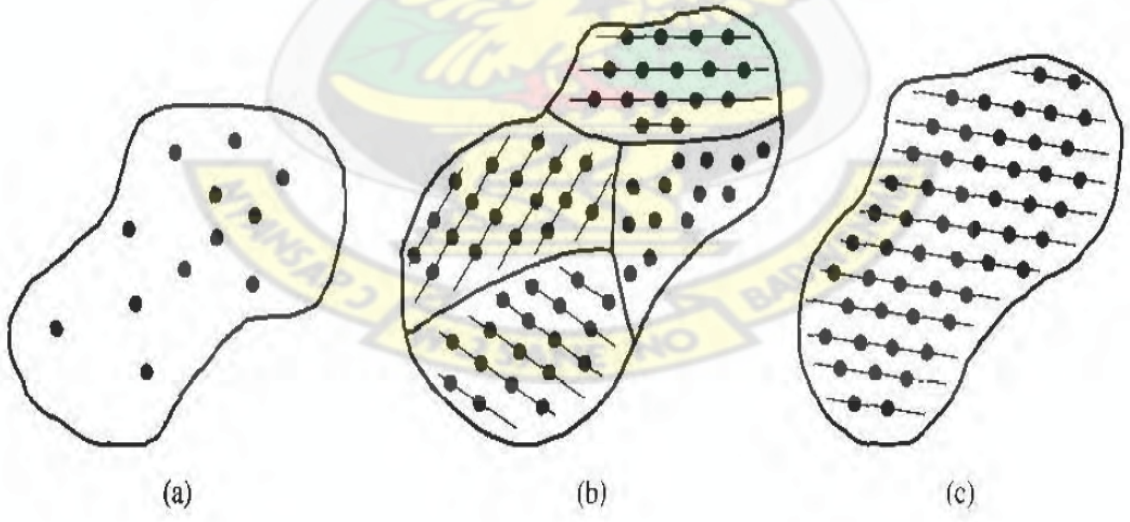

Figure 3.1 Schematics of the three general types of structural orders: (a) amorphous, (b) polycrystalline, (c) crystalline.

3.0.1. CRYSTALLINE SEMICONDUCTORS

In crystalline materials, the atoms are arranged in a periodic, regularly repeated three-dimensional pattern—thus presence of long-range order. The universe of traditional solid state physics is defined by the crystalline lattice. The principal actors are the elementary excitations like phonons, polarons, magnons etc. in this lattice. Another is the electron that is perhaps the principle actor in all of solid state physics. By electron in a solid we mean something a little different from a free electron (Petterson and Bailey, 2005).

A. H. Wilson showed in 1931 how the electronic band theory of crystals developed by F. Bloch can be applied to the understanding of semiconductors. Properties such as the negative temperature coefficient of electrical resistivity follow naturally from Wilson's theory. The key ingredients are the Bloch states which are the eigenstates of an electron moving in the periodic potential of a crystal. The energies of the Bloch states cannot take on all possible values, but are restricted to certain allowed regions or bands separated from one another by forbidden regions called band gaps or energy gaps. Band theory and its outcome-effective mass theory-has allowed us to understand the difference between metals, insulators and semiconductors and how electrons respond to external forces in solids (Balkanski and Wallis, 2000; Singh, 2003)

Information about the structure of solids can be obtained by plotting the so-called radial distribution function, which is the probability, *P(r)*, of finding an atom at a distance *r* from a given atom. In crystalline solids, such a radial distribution function exhibits series of sharp peaks indicative of the long-range order. The curve representing an amorphous

material indicates the presence of the short-range order only. This also implies that the number of nearest neighbors to any given atom, on average, is not much different from the corresponding number in the crystalline material.

The electronic band structure of crystalline semiconductors is substantially different from that in the amorphous semiconductors. In crystalline materials, the periodicity of the atomic structure and the presence of long-range order result in a band structure with allowed and forbidden electronic levels, with sharp band edges and a fundamental energy gap separating valence band from the conduction band. In amorphous semiconductors, there is still a fundamental energy gap based on the short-range bonding between the atoms; however, the sharp band edges of the crystalline semiconductor are replaced in the amorphous materials by exponential band tails due to localised states related to the structural disorder (i.e., bond length and bond angle deviations that broaden the distribution of electronic states); in addition, defects (i.e., dangling bonds) introduce electronic levels in the energy gap (Yacobi, 2004). From observations and measurements we find that it is the regular crystalline structure that leads to certain special properties and behaviour of the associated materials (Korvink, and Greiner, 2002). The advantage of crystalline material is that, in general, its electrical properties are superior to those of a nonsingle-crystal material, since grain boundaries tend to degrade the electrical characteristics (Neamen, 2003).

3.0.2. POLYCRYSTALLINE SEMICONDUCTORS

In polycrystalline materials, numerous crystalline regions called grains, have different orientation and are separated by a grain boundary**.** That is, they have a high degree of order over many atomic or molecular dimensions. These ordered regions or single-crystal regions only vary in size and orientation with respect to one another (Neamen, 2003).

These semiconductors can be further classified as (i) microcrystalline and nanocrystalline materials that are usually prepared as thin films and (ii) large grain materials in the form of sliced ingots and sheets. The grain size in polycrystalline materials depends on the substrate temperature during thin film growth, the thickness of the film and also on post-growth annealing treatment of the film. It is important to consider here that many solids are incorrectly described as being amorphous, but are in fact microcrystalline or nanocrystalline with small crystallite sizes which fail to give crystalline X-ray diffraction patterns. However, often these materials can be confirmed as crystalline using electron diffractions, with lattice images routinely obtained from particles in the range of 5 nm. The grain boundaries generally have an associated space-charge region controlled by the defect structure of the material and the grain boundaries are paths for the rapid diffusion of impurities affecting various properties of polycrystalline materials. An important consequence of the presence of potential barriers on grain boundaries in a polycrystalline semiconductor is the increase of its electrical resistivity. One of the important processes is the decoration of grain boundaries, that is, the process in which precipitates of impurity elements segregate to the boundaries.

In general, the grain boundaries introduce allowed levels in the energy gap of a semiconductor and act as efficient recombination centers for the minority carriers. This effect is important in minority-carrier devices, such as photovoltaic solar cells and it is expected that some of the photogenerated carriers to be lost through recombination on the grain boundaries. Typically, the efficiency of the device will improve with increasing grain size. In this context, the columnar grain structure (i.e. grains in a polycrystalline material extend across the wafer thickness) is more desirable as compared to the material containing fine grains that do not extend from back to front of a device structure. In order to prevent significant grain boundary recombination of the minority carriers, it is also desirable that the lateral grain sizes in the material be larger than the minority carrier diffusion length. It should also be mentioned that the possible preferential diffusion of dopants along the grain boundaries and or precipitates of impurity elements segregated at the boundaries may provide shunting paths for current flow across the device junction.

It should also be noted that hydrogen passivation of grain boundaries in polycrystalline silicon devices, such as photovoltaic cells, is an effective method of improving their photovoltaic performance efficiency. This improvement is associated with the mechanism similar to that of the passivation of dangling bonds in amorphous silicon (Yacobi, 2004; Gellings and Bouwmeester, 1997)

3.0.3. AMORPHOUS SEMICONDUCTORS

In contrast to crystalline materials amorphous semiconductors have only short-range order with no periodic structure see Figure 3.3. These materials can be relatively, inexpensively produced as thin films deposited on large area substrates (Yacobi, 2004).

An interesting aspect of thin film deposition techniques is that they facilitate the formation of amorphous metal and semiconductor structures relative to bulk preparation methods (Ohring, 1992).

What happens to the electron energy band model in a solid without regular crystalline order? The Bloch theorem is not applicable when the structure is not periodic, so that the electron states cannot be described by well-defined $\boldsymbol{k}$ values. Thus, the momentum selection rule for optical transitions is relaxed; hence all infrared and Raman modes contribute to the absorption spectra. The optical absorption edge is rather featureless. And since momentum conservation rules or direct and indirect optical transitions no longer apply, in the case of amorphous silicon, e.g., this results in very high absorption coefficient, allowing the use of only micrometer scale thin films for absorption of solar energy. As previously noted, allowed bands and energy gaps still occur because the form of the density of states (DOS) versus energy is determined most strongly by local electron bonding configurations.

In amorphous semiconductors, charge carriers may be scattered strongly by the disordered structure, so that the mean free path may sometimes be of the order of the scale of the disorder. Anderson (1958) proposed that the states near the band edges may be localised and do not extend through the solid. It should be noted that the transition from the localised states to the extended states results in a sharp change in the carrier mobility, leading to the presence of the mobility edges or the mobility gap. The carrier mobility in the extended states is higher and the transport process is analogous to that in crystalline materials; whereas in the localised states, the mobility is due to thermally-activated tunneling between those states (i.e., hopping conduction) and it is lower as

compared to the extended states. Thus, Anderson localization transition caused by random local field fluctuations due to disorder can lead to “mobility edges” rather than band edges as illustrated in Figure 3.2 and hence, rather than an energy gap one has a mobility gap separating localised and nonlocalised or extended states (Kittel, 2005; Yacobi, 2004; Petterson and Bailey, 2005)

Two distinct classes of amorphous semiconductors are widely studied: tetrahedrally-bonded amorphous solids such as silicon and germanium and chalcogenide glasses. The latter are multicomponent solid of which one major constituent is a “chalcogen” element—sulphur, selenium, or tellurium (Kittel, 2005).

The tetrahedrally-bonded materials have properties similar to those of their crystalline forms, provided the dangling bonds defects are compensated with hydrogen. They can be doped with small amount of chemical impurities and their conductivity can be sharply modified by injection of free carriers from a metallic contact. By contrast, the chalcogenide glasses are largely insensitive to chemical impurities and to free carrier injection.

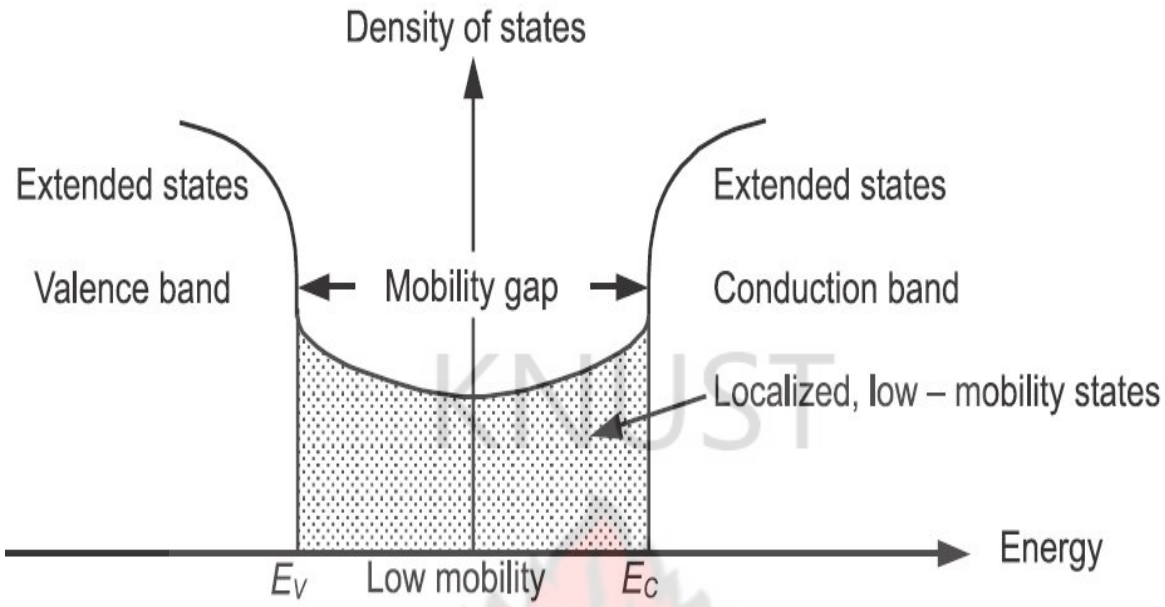

Figure 3.2 Area of mobility between valence and conduction bands

In amorphous materials, defects are of different kind as compared to crystalline materials. In the case of amorphous materials, the main defects are those related to the deviations from the average coordination number, bond length and bond angle; other defects include, e.g., dangling bonds, deviations from an optimal bonding arrangement and microvoids.

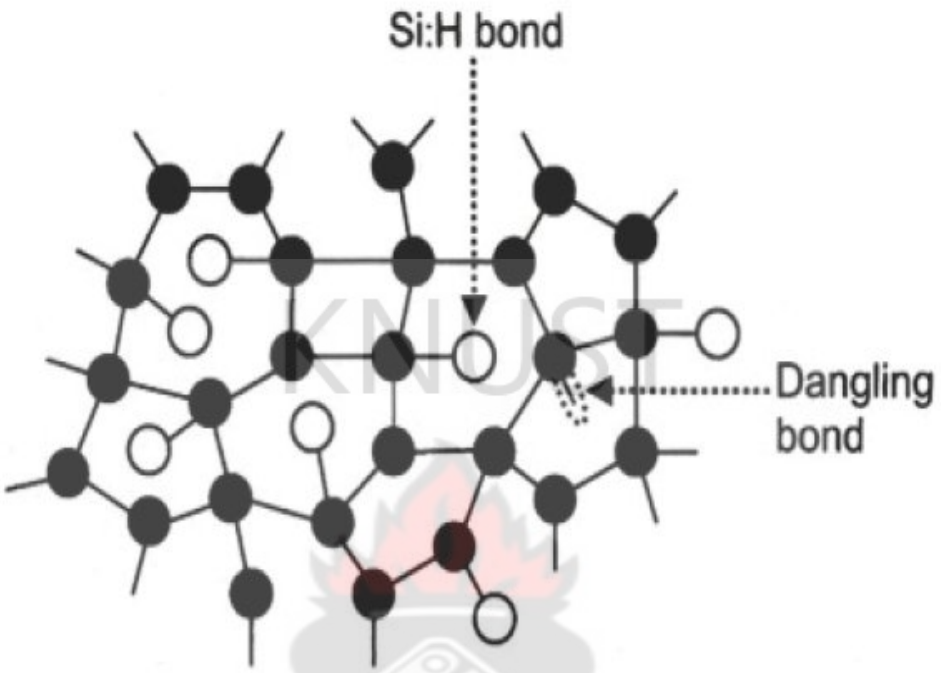

Figure 3.3 Schematic illustration of a two-dimensional continuous random network of atoms having various bonding coordination.

As mentioned above, in amorphous semiconductors, the allowed energy bands have band tails in the energy gap (Yacobi, 2004). Consider a degenerate direct band gap p-type semiconductor. One can excite electrons from states below the Fermi level, E_f, in the valence band where the band is nearly parabolic, to tail states below conductions band edge, E_c, where the density of states decreases exponentially with energy into the band gap, away from E_c. Such excitations lead to absorption coefficient, α, depending

exponentially on photon energy, hv, a dependence that is usually called the Urbach rule, given by

$$\alpha=\alpha_0 \exp\left[(hv-E_0)/\Delta E\right] \qquad (3.0.1)$$

where α_0 and E_0 are material- dependent constants and ΔE, called the Urbach width, is also a material-dependent constant. The Urbach rule was originally reported for alkali halides. It has been observed for many ionic crystals, degenerately doped crystalline semiconductors and almost all amorphous semiconductors. While exponential band tailing can explain the observed Urbach tail of the absorption coefficient vs. photon energy, it is also possible to attribute the absorption tail behaviour to strong internal fields arising, for example, from ionized dopants or defects. Temperature-induced disorder in the crystal is yet another important mechanism that leads to an Urbach exponential absorption tail (Singh, 2006). The typically observed exponential energy dependence of the absorption edge or the Urbach edge provides an important parameter for characterizing the material's quality and it usually depends on the deposition method and deposition conditions. Thus as already noted above, in amorphous materials the exponential band tails are related to the structural disorder, i.e., bond length and bond angle deviations that broaden the distribution of electronic states; hence, the slope of the Urbach edge can be related to the material's quality (Street, 1991).

3.1. OPTICAL PROPERTIES OF FILM MATERIALS

Optical properties of semiconductors typically consist of their refractive index n and extinction coefficient k or absorption coefficient α (or equivalently the real and imaginary parts of the relative permittivity) and their dispersion relations, that is their dependence

on the wavelength, λ, of the electromagnetic radiation or photon energy *hv*, and the changes in the dispersion relations with temperature, pressure, alloying, impurities, etc. A typical relationship between the absorption coefficient and photon energy observed in a crystalline semiconductor is shown in figure 3.4, where various possible absorption processes are illustrated (Singh, 2006). The important features in the α vs. *hv* behaviour as the photon energy increases can be classified in the following types of absorptions: (a) Reststrahlen or lattice absorption in which the radiation is absorbed by vibrations of the crystal ions, (b) free-carrier absorption due to the presence of free electrons and holes, an effect that decreases with increasing photon energy, (c) an impurity absorption band (usually narrow) due the various dopants, (d) exciton absorption peaks that are usually observed at low temperatures and are close to the fundamental absorption edge and (e) band-to-band or fundamental absorption of photons, which excites an electron from the valence to the conduction band (Singh, 2006).

The fundamental absorption process, probably the most important absorption effect, involves the absorption of photons, which have energies equal to or greater than the band gap energy. The fundamental absorption process is usually accompanied by an electronic transition across the forbidden gap and as a result, excess electron-hole pairs are generated in the semiconductor. The fundamental absorption manifests itself by a rapid rise in absorption and can be used to determine the band-gap energy of semiconductors and insulators.

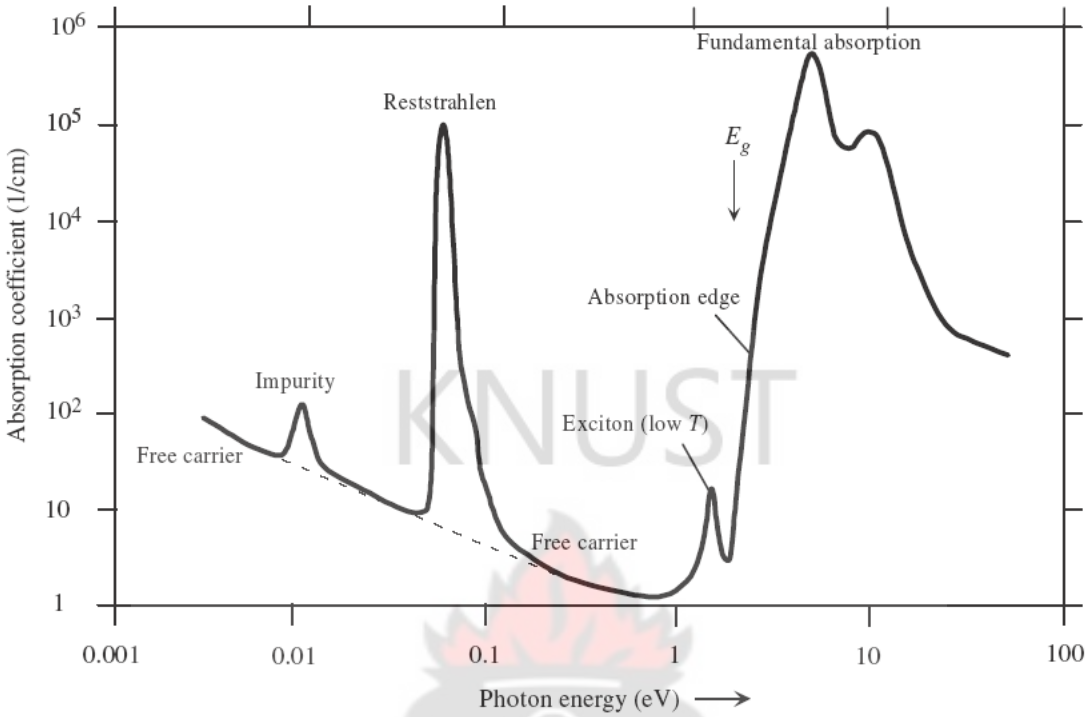

Figure 3.4 Absorption coefficient is plotted as a function of the photon energy in typical semiconductor to illustrate various possible absorption processes.

The absorption coefficient due to the interband transition is usually very large. However, the absorption coefficient becomes very small (<1 cm^{-1}) when the photon energies fall below the band gap energy. In this case, another type of optical absorption process takes place which results in electronic transitions only within the allowed energy band and is called the free-carrier absorption process. This type of absorption result in the excitation of lattice phonons, accelerate free electrons in the conduction band or creation of an exciton (Li, 2006).

In order to understand the optical behaviour of films, one must become familiar with the optical constants of materials, their origins, magnitudes and how they depend on the way

films are processed. The unifying concept that embraces all optical properties is the interaction of electromagnetic radiation with the electrons of the material. On this basis, optical properties are interpretable from what we know of the electronic structure and how it is affected by atomic structure, bonding, impurities, and defects (Ohring, 1992).

3.1.1. OPTICAL MAGNITUDES AND THE DIELECTRIC CONSTANTS

Electromagnetic radiation propagates differently in materials than in free space because of the presence of charge. As a result, there is a change in the wave velocity and intensity of the radiation described by the complex index of refraction

$$N = n - ik \quad \text{s} \tag{3.1.1}$$

The quantity n is the real index of refraction and k is the index of absorption, which is also known as the extinction coefficient. These are the two material optical constants of concern here. The spatially dependent portion of the electric field of a wave propagating in the x direction is then expressed by.

$$E = E_0 \exp-(\frac{i2\pi Nx}{\lambda}) = E_0 \exp-\frac{2\pi kx}{\lambda} \exp-\frac{i2\pi nx}{\lambda} \tag{3.1.2}$$

Where E_0 is the field amplitude when x = 0 and λ is the wavelength. The real function $\exp- 2\pi kx/\lambda$ represents an exponential damping or attenuation of the wave due to some absorption process within the material. On the other hand, the imaginary exponential portion of Eq. (3.1.2) contains *n* and reflects propagation without absorption. All materials exhibit varying proportion of these two linked attributes of N. In the highly absorbing metals, for example, *n* is usually small compared with *k*. On the other hand, the dielectric films used for optical purposes are highly non-absorbing and *k* is vanishingly

small compared with n. Multiplying E by its complex conjugate leads to the well-known expression for the attenuation of the intensity, $I \propto EE^*$ or $I \propto E_0^{\,2} \exp -4\pi kx/\lambda$. therefore (Ohring, 1992).,

$$I = I_0 \exp -\alpha x \tag{3.1.3}$$

where the absorption coefficient α is defined as $4\pi k/\lambda = 2\omega k/c$ and I_0 is the intensity of incident radiation, c is the speed of light.

Of the total radiation energy incident on an object, a fraction R is reflected from the top surface and a fraction T is transmitted through the bottom surface. The remaining fraction is lost through electronic absorption (A) processes and by scattering (S) at surface and volume imperfections. Surface roughness, internal boundaries and density fluctuations arising from porosity, pinholes, microcracks, particulate incorporation and impurities are sources of scattering. Adding the various contributions gives

$$R + T + A + S = 1 \tag{3.1.4}$$

For light passing through a medium of refractive index n_0, impinging normally on a transparent film of index n_1,

$$R = \left(\frac{n_1 - n_0}{n_1 + n_0}\right)^2 \tag{3.1.5}$$

If, however, the film is absorbing with index of absorption k_1

$$R = \frac{(n_0 - n_1)^2 + k_1^2}{(n_0 + n_1)^2 + k_1^2} \tag{3.1.6}$$

The well known Maxwell's formula for the refractive index of a substance is $N = \sqrt{\varepsilon\ \mu}$, where ε is the static dielectric constant or relative permittivity and μ the relative permeability. As $\mu = 1$ for nonmagnetic substances, one gets $N = \sqrt{\varepsilon}$. As ε depends on the wavelength of light, the refractive index also depends on the wavelength of light, and this dependence is called dispersion. The complex refractive index is related to the complex relative permittivity, $N = n - ik = \sqrt{\varepsilon} = \sqrt{\varepsilon_1 - i\varepsilon_2}\ \ \varepsilon = \varepsilon_1 - i\varepsilon_2$, (3.1.7)

where ε_1 and ε_2 are, respectively, the real and imaginary parts of ε. It can be deduced that

$$n^2 - k^2 = \varepsilon_1 \text{ and } 2nk = \varepsilon_2 \qquad (3.1.8)$$

In explicit terms, *n* and *k* can be obtained as (Singh, J., 2006):

$$n = \left[1/2\left(\left(\varepsilon_1^2 + \varepsilon_2^2\right)^{1/2} + \varepsilon_1\right)\right]^{1/2} \qquad (3.1.9)$$

$$k = \left[1/2\left(\left(\varepsilon_1^2 + \varepsilon_2^2\right)^{1/2} - \varepsilon_1\right)\right]^{1/2} \qquad (3.1.10)$$

3.1.2. ELECTRONIC TRANSITIONS IN SEMICONDUCTORS

There are two types of optical transition associated with the fundamental absorption process, namely, direct and indirect band-to-band transitions, as shown in Figure 3.5a and b. Since the photon momentum is small compared with the crystal momentum, the

absorption process should essentially conserve the electron momentum, i.e., $\hbar k$. The direct (or vertical) transition shown in Figure 3.5a is the dominant absorption process taking place in a direct band gap semiconductor like GaAs, where the conduction band minimum and the valence band maximum are located at the same k-value in the reciprocal space. For an indirect band gap semiconductor (e.g., Si, Ge), the conduction band minimum and the valence band maximum are not located at the same k-value in the reciprocal space as shown in Figure 3.5b. Therefore, the indirect optical transition induced by photon absorption is usually accompanied by the simultaneous absorption or emission of a phonon to conserve momentum; the probability of such a process is substantially lower compared with direct transitions (Li, 2006). Therefore, in general, fundamental absorption in indirect gap semiconductors is relatively weaker as compared with the direct gap materials.

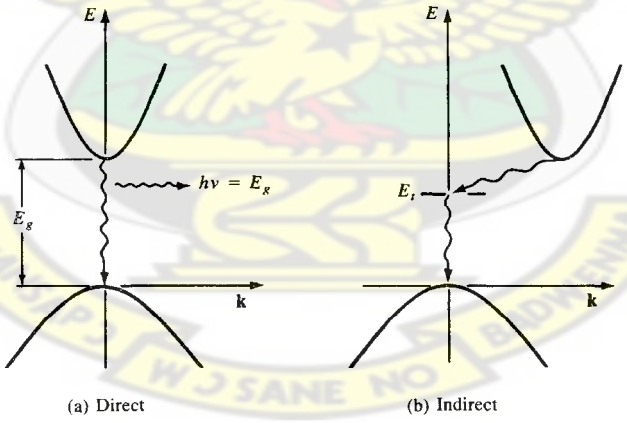

Figure 3.5 Direct and indirect electron transitions in semiconductors (a) Direct transition with accompanying photon emission; (b) indirect transition via a defect level.

3.1.3 IMPURITY ABSORPTION

Impurity absorption can be registered as the peaks of absorption coefficient lying below the fundamental (band-to-band) and excitonic absorption. Mostly they can be related to

the presence of ionized impurities or, simply, ions. The origin of these peaks lies in the electronic transitions either between electronic states of an ion and conduction/valence band or intra-ionic transitions (e.g., within d or f shells, or between s and d shells, etc.). In the first case the appearing features are intense and broad lines while in the latter case their appearance strongly depends on whether these transitions are allowed or not by the parity selection rules. For allowed transitions the appearing absorption peaks are quite intense and broad while the forbidden transitions produce weak and narrow peaks. **(**Singh, 2006)

3.1.4. OPTICAL ABSORPTION AND BAND GAP

The optical absorption is described by an absorption coefficient α, which can be derived from transmission or absorption measurements. If I_0 is an incident light intensity, I is the transmitted light intensity and R is the reflectivity, then the transmission, $T = I/I_0$ can be written as (neglecting interference)

$$T = \frac{(1-R)^2 \exp(-\alpha t)}{1-R^2 \exp(-2\alpha t)} \tag{3.1.11}$$

where t is the thickness of the material. For large αt, this expression can be reduced to

$$T = (1-R)^2 \exp(-\alpha t) \tag{3.1.12}$$

and, in the absence of reflection, it can be further reduced to

$$I = I_0 \exp(-\alpha t) \tag{3.1.13}$$

In terms of absorbance A,

$$\alpha = \frac{1}{t}(2.303A) \tag{3.1.14}$$

The relation between the absorption coefficient and the incident photon energy in a direct transition is given by

$$\alpha h\nu = A(h\nu - E_g)^n \tag{3.1.15}$$

where A is a constant, E_g is the optical energy gap. The value of n is $1/2, 3/2$ for direct allowed and direct forbidden transitions respectively. Thus, a plot of $(\alpha h\nu)^2$ versus $h\nu$ allows one to determine the energy gap (Tauc, 1974; Yacobi, 2004).

The optical absorption coefficient due to the indirect transitions with phonon absorption is

$$\alpha_a = \frac{A(h\nu - E_g + E_p)^2}{(\exp(E_p / k_B T) - 1)} \tag{3.1.16}$$

E_p is the phonon energy. Similarly, for transitions involving phonon emission is

$$\alpha_e = \frac{A(h\nu - E_g + E_p)^2}{(1 - \exp(-E_p / k_B T))} \tag{3.1.17}$$

meaning the optical absorption coefficient for the indirect allowed transitions varies with the square of the photon energy. A plot of α^2 versus $h\nu$ at different temperatures should yield a straight line, and its intercept with the horizontal axis allows one to determine the photon energy and the energy band gap of a semiconductor.

CHAPTER FOUR

4. EXPERIMENTAL DETAILS

4.0 REAGENTS

The chemicals used for the film preparation, as well as their source and percentage purity are listed as follows:

- Zinc Chloride, $ZnCl_2$ (BDH, Percentage purity = 98.0 %)
- Thioacetamide, C_2H_5NS (LABOSI, Percentage purity = 98.0 %)
- Urea, NH_2CONH_2 (M&B, Percentage purity = 99.0 %)

4.0.1 PREPARATION OF 0.15 M $ZnCl_2$ (ZINC CHLORIDE)

2.00 g of $ZnCl_2$ was weighed into a beaker. The salt was dissolved in small amount of distilled water and then transferred into 100 ml volumetric flask using funnel. The solution was then topped up to the 100 ml mark with distilled water and thoroughly shaken to dissolve the salt completely. The resulting solution had a concentration of 0.15 M.

4.0.2 PREPARATION OF 5.0 M NH_2CONH_2 (UREA)

29.73 g of NH_2CONH_2 was weighed into a beaker. The salt was dissolved in small amount of distilled water and then transferred into 100 ml volumetric flask using funnel. The solution was then topped up to the 100 ml mark with distilled water and thoroughly shaken.

4.0.3 PREPARATION OF 1 M CH_3CSNH_2 (THIOACETAMIDE)

3.68 g of CH_3CSNH_2 was weighed into a beaker. The salt was dissolved in small amount of distilled water and then transferred into 50 ml volumetric flask using funnel. The solution was then topped up to the 50 ml mark with distilled water and thoroughly shaken.

4.1. SURFACE PREPARATION OF SUBSTRATES

A clean surface is one that contains no significant amount of undesirable material (Mattox, 1978). Cleaning is defined as the removal, by physical and or chemical means, of soil that could interfere with the preparation of the desired material. Soil is matter on the surface whose chemical characteristics are different from those being formed. The types of soils most commonly encountered are fingerprint oils, metal oxides, dirt, etc. (Beal, 1978). The nature and surface finish of the substrates are extremely important because they greatly influence the properties of films deposited on them (Chopra, 1969). It is therefore important that prior to the deposition of the semiconducting thin film the substrate, in this case, microscope glass slide is cleaned thoroughly to remove any undesirable substance from it. The glass slides were left in a solution of Aqua Regia (3 parts HCl: 1 part HNO_3), for about 24 hours to remove any grease. They were then cleaned with detergent and rinsed with distilled water before use.

4.2. PREPARATION OF THE THIN FILM

In a typical experiment thin films of ZnS were grown on silica glass substrates from acidic baths (pH 5) containing solutions of zinc chloride (0.15 M), Urea (5.0 M) and thioacetamide (0.1 M). The stirred reaction mixture was maintained at a temperature of 353 K for deposition. Substrates were degreased and cleaned thoroughly by ultrasonication using a standard procedure, before immersion in the chemical bath. Substrates were removed from the bath after 2 hours, washed in de-ionised water and any adherent particulate matter removed by ultrasonic agitation. As deposited films were whitish in colour and adherent. The substrates were allowed to dry under ambient conditions before film characterization or a further annealing step.

4.2.1 REACTION MECHANISM

The deposition process is based on the slow release of Zn^{2+} and S^{2-} ions in solution which then condense on the substrate. The deposition of ZnS occurs when the ionic product of Zn^{2+} and S^{2-}exceeds the solubility product of ZnS (Antony *et al*., 2005).

$ZnCl_2$ is used as the Zn^{2+} source and thioacetamide supplies S^{2-} ions through hydrolysis in an acidic medium according to the following equations:

$$ZnCl_2 \longrightarrow Zn^{2+} + 2Cl^- \qquad 3.1$$

$$CH_3SCNH_2 + H_2O \rightleftharpoons S^{2-} + CH_3CONH_2 + 2H^+ \qquad 3.2$$

Urea hydrolyze in an acidic medium to produce ammonia which forms a complex ion with Zn^{2+} according to:

$$CO(NH_2)_2 + H_2O \rightleftharpoons 2NH_3 + CO_2 \qquad 3.3$$

$$Zn^{2+} + 4NH_3 \rightleftharpoons [Zn(NH_3)_4]^{2+} \qquad 3.4$$

From equations (3.2) and (3.4), the complex and sulfide ions migrate to the substrate surface, where they react to form ZnS:

$$Zn(NH_3)_4^{2+} + S^{2-} \rightleftharpoons ZnS + 4NH_3 \qquad 3.5$$

Assuming the metallic complex of the form ZnL_n^{2+}, where L is the complexing agent, the general reaction for the ZnS deposition can be represented as:

$$ZnLn^{2+} + CH_3SCNH_2 + H_2O \xrightarrow{H^+} ZnS(substrate) + nL + CH_3CONH_2 + 2H^+ \qquad 3.6$$

Hence:

$$Zn(NH_3)_4^{2+} + CH_3SCNH_2 + H_2O \xrightarrow{H^+} ZnS(substrate) + 4NH_3 + CH_3CONH_2 + 2H^+ \qquad 3.7$$

During the deposition of ZnS thin films, according to the reactions (3.5), the formation of $Zn(OH)_2$ occurs as a competitive process in the bath. So we can expect that the Zn^{2+} ions have to be in form of $Zn(OH)_2$ precipitate, however it is not true due to the presence of NH_3 which forms with Zn^{2+}, the complex $Zn(NH_3)_4$ which is soluble in this medium (Ubale *et al*., 2005).

The thickness of the deposited films was measured by the gravimetric method using a sensitive electronic balance.

4.2.2 CHARACTERIZATION OF THIN FILMS

Optical absorption spectra were recorded with a Schimadzu UV-VIS spectrophotometer (model: UV mini-1240) within the wavelength range of 200–800 nm, at room temperature. X-ray diffraction studies were performed using secondary graphite

monochromated Cu-Kα radiation (40 kV) on a Philips X'Pert materials Research Diffractometer. Energy dispersive analytical x-ray analysis (EDAX) and Scanning electron microscopy (SEM) measurements were also conducted.

4.3. THE MEASUREMENT OF ABSORPTION SPECTRA

Absorption spectra are usually registered by instruments known as spectrophotometers. Figure 4.2 shows a schematic diagram with the main elements of the simplest spectrophotometer. Basically, it consists of the following components: (i) a light source (usually a deuterium lamp for the UV spectral range and a tungsten lamp for the VIS and IR spectral ranges) that is focused on the entrance to (ii) a monochromator, which is used to select a single wavelength (frequency) from all of those provided by the lamp source and to scan over a desired frequency range. (iii) a sample holder, followed by (iv) a light detector, to measure the intensity of each monochromatic beam after traversing the sample and finally (v) a computer, to display and record the absorption spectrum (Sole, *et al*., 2005).

The Schimadzu UV-VIS spectrophotometer (model: UV mini-1240) used in this work. A glass slide that had been treated the same way as the slides with films but with no film on it was used as the reference slide. The wavelength was varied in units of 10 from 200 nm to 800 nm and the corresponding absorbance reading recorded.

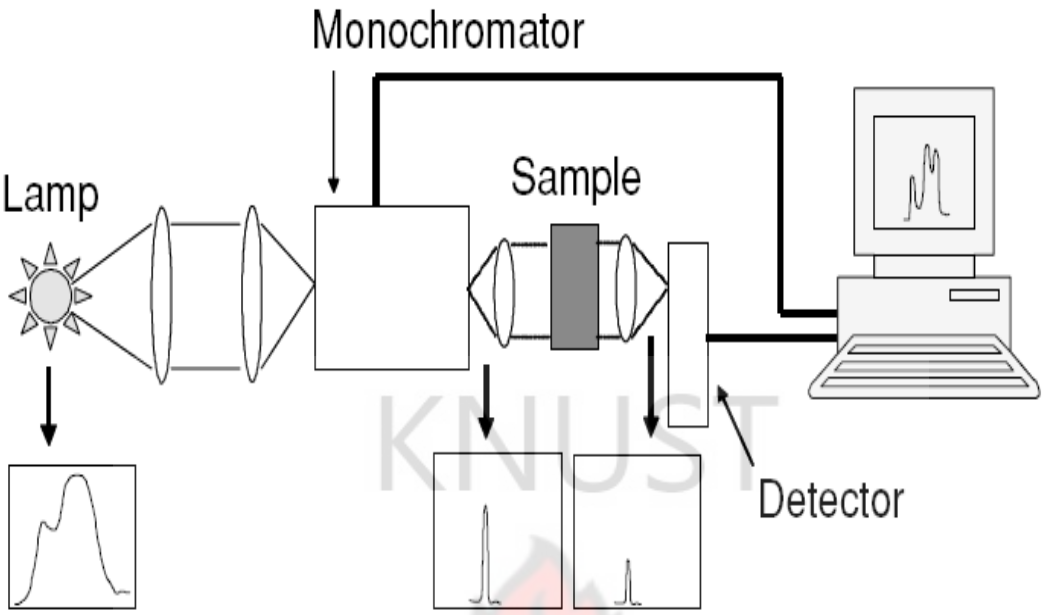

Figure 4.2 Schematic diagram of a single-beam spectrophotometer.

Aside the absorbance of the as deposited films, the samples were thermally annealed for one hour at temperatures of about 300 °C, 400 °C, 500 °C and the absorbance again recorded.

4.4. THE MEASUREMENT OF FILM THICKNESS

The thickness of a film is among the first quoted attributes of its nature. The reason is that thin film properties and behaviour depend on thickness. Decorative, metallurgical, protective films and coatings are some applications where film thickness is not particularly crucial to function. On the other hand, microelectronic applications generally require the maintenance of precise and reproducible film thicknesses as well as lateral

dimensions. Even more stringent thickness requirements must be adhered to in optical applications, particularly in multilayer coatings (Ohring, 1992).

The varied types of films and their uses have generated a multitude of ways (optical and mechanical) to measure film thickness. A list of some methods is given in Table 4.1 with typical measurement ranges and accuracies. Included are destructive and nondestructive methods. The overwhelming majority are applicable to films that have been prepared and removed from the deposition chamber. Only a few are suitable for real-time monitoring of film thickness during growth (Ohring, 1992).

Table 4.1 A Summary of Selected Film Thickness Measurement Techniques

Method	Range	Accuracy or Precision	Comments
Multiple-beam FET	30–20,000 Å	10–30 Å	A step and reflective coating required
Multiple-Beam FECO	10–20,000 Å	2 Å	A step, reflective coating, and spectrometer required; accurate but time-consuming
VAMFO	800 Å–10 μm	0.02–0.05 %	For transparent films on reflective substrates; Nondestructive
CARIS	400 Å–20 μm	10 Å–0.1%	For transparent films; Nondestructive
Step gauge	500–15,000 Å	~ 200 Å	Values for SiO_2 on Si
Ellipsometry	A few Å to a few μm	1 Å	Transparent films; complicated mathematical analysis
Stylus	20 Å to no limit	A few Å to < 3%	Step required; simple and rapid
Weight measurement	< 1 Å to no limit		Accuracy depends on knowledge of film density
Crystal oscillator	< 1 Å to a few μm	< 1 Å to a few %	Nonlinear behavior at larger film thicknesses

In this work the weight measurement method also called gravimetric technique was employed because of the lack of film thickness measuring equipment such as interferometers or stylus instruments. Knowing the film mass *m*, the deposit area *A*, and the film density ρ, the thickness t, is given as

$$t = \frac{m}{\rho A} \qquad (4.4.1)$$

To know the film mass means weighing the substrate before and after deposition and subtracting the mass before deposition from the mass after deposition with a precision mass balance. This method has a number of challenges in measuring film thickness because film density is not known with certainty. The reason is that the film packing factor P, a measure of the void content, can be quite low for porous deposits. Furthermore, the effective deposit area will be larger than the assumed in case the substrate contains a great deal of relief in the form of roughness, cleavage steps etc.

CHAPTER FIVE

5.0 RESULTS AND DISCUSSION

5.0.1. ABSORBANCE

As deposited thin films were whitish in colour and adherent. The Figures (5.1A-5.1D) below show the absorption spectra of thin films of ZnS before and after annealing at temperatures of 300 °C, 400 °C and 500 °C.

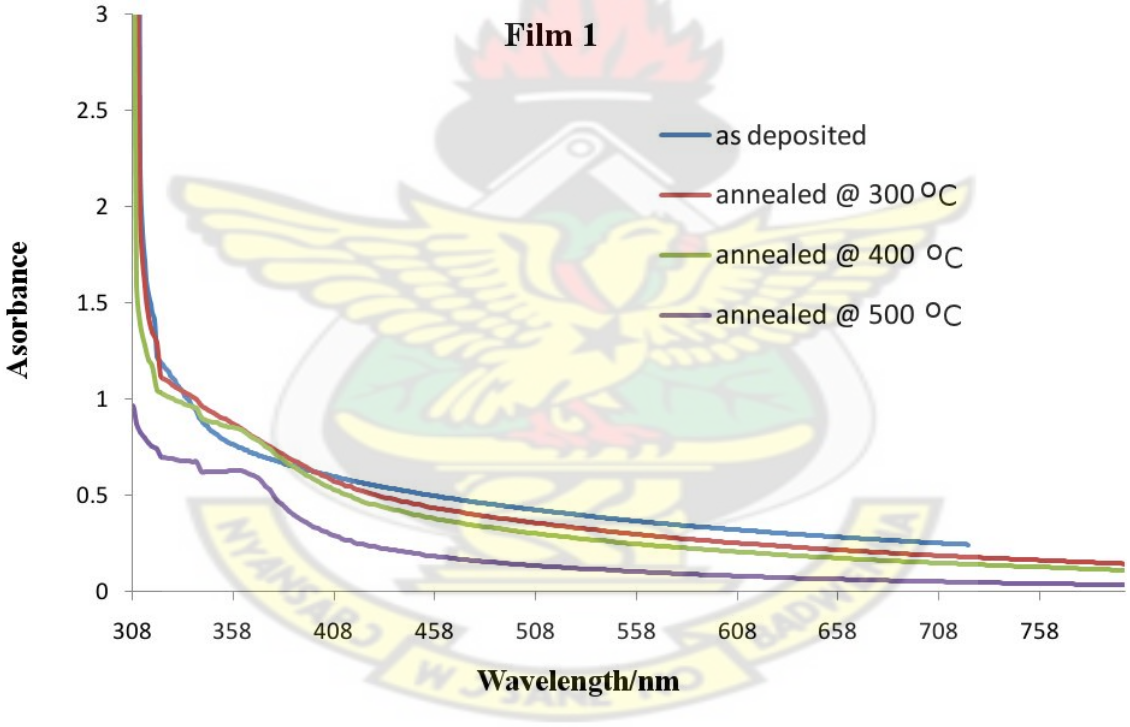

Figure 5.1A A plot of absorbance versus wavelength showing absorbance dependence of annealing temperature of Sample 1 with thickness 684 nm.

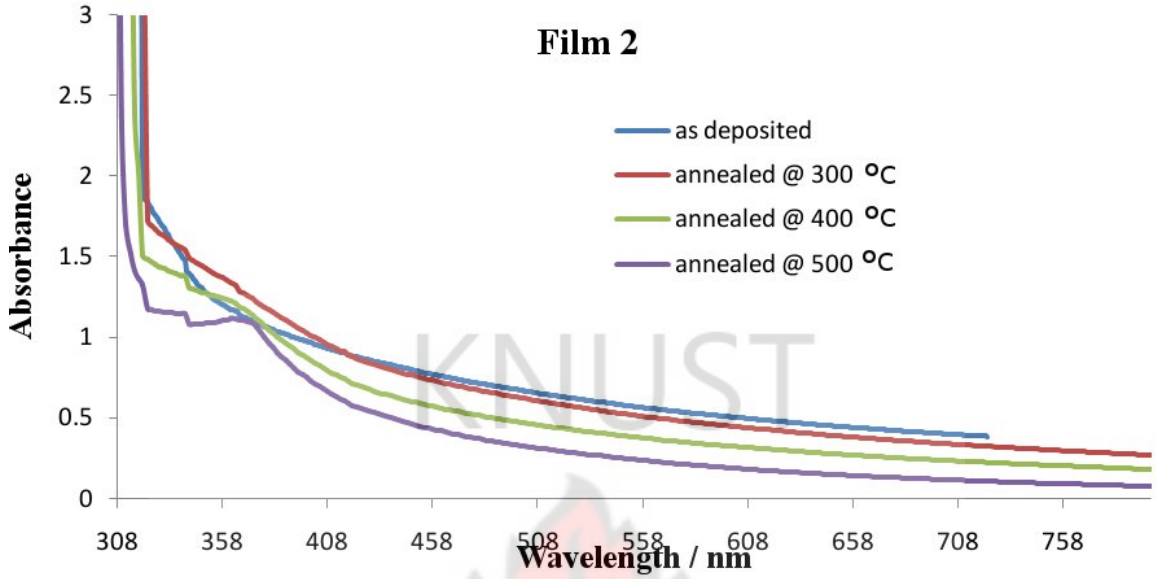

Figure 5.1B A plot of absorbance versus wavelength showing absorbance dependence of annealing temperature of Sample 2 with thickness 572 nm.

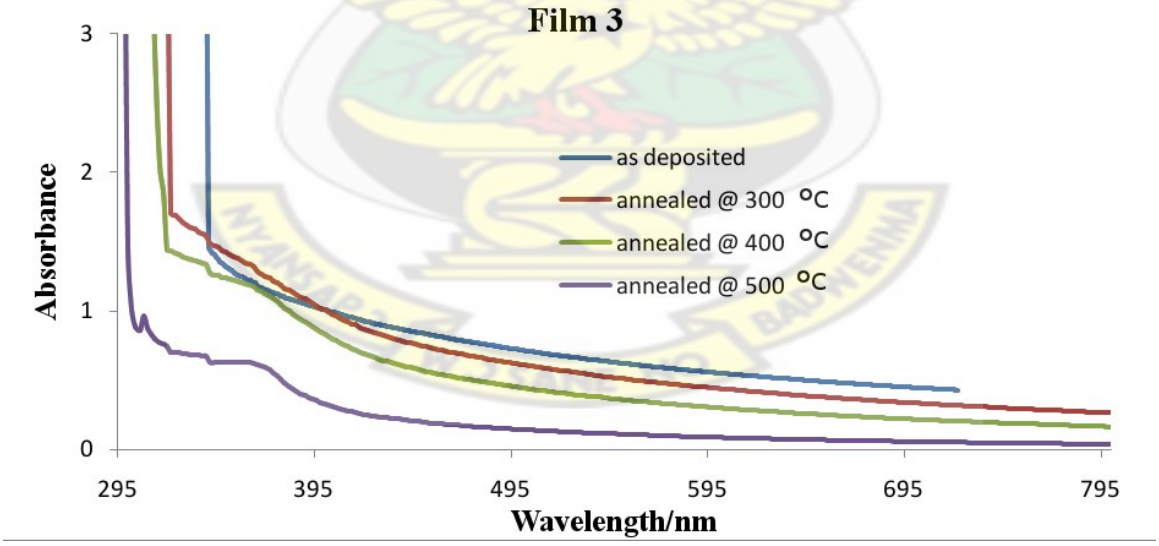

Figure 5.1C A plot of absorbance versus wavelength showing absorbance variation of annealing temperature of Sample 3 with thickness 523 nm.

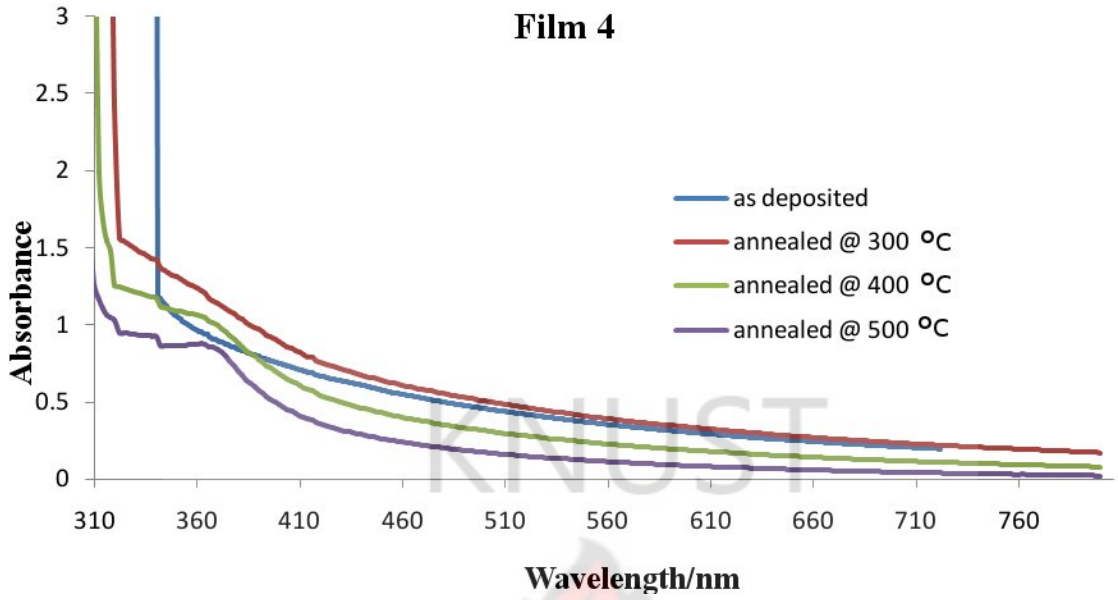

Figure 5.1D A plot of absorbance versus wavelength showing absorbance dependence of annealing temperature of Sample 4 with thickness 270 nm

It can be observed that above the 400 nm wavelength, the absorbance of the samples are low and lie between 0 and 1.0.

The films show a marginal decrease in absorbance after annealing and this might be attributed to the improvement in crystallinity in the films with increasing annealing temperature (Melin *et al.,* 2009). Annealing the samples could lead to minimizing structural imperfections in the prepared thin films resulting in fewer states within the band gap available for photon absorption. Hence, lower absorbance readings.

The decrease in absorbance with increasing annealing temperature may also be due to diffusion of Zn into glass (Zendehnam et al, 2010). It can be observed that the fundamental absorption edge of the samples shift towards shorter wavelengths with

increasing annealing temperatures. This shift indicates an increase of the optical band gap which is also evidence of reduction in the tail states present within amorphous semiconductors as proposed by Mott (1970).

5.0.2 TRANSMITTANCE

When light is incident on a material, fraction of the light beam that is not reflected or absorbed is transmitted through the material.

Transmission data was obtained from the absorption spectra by the relation: $= 10$ where T is the transmittance and A is the absorbance. The Figures below (Figure 5.2A-5.2D) show the transmission spectra of ZnS thin films as deposited and annealed at different temperatures.

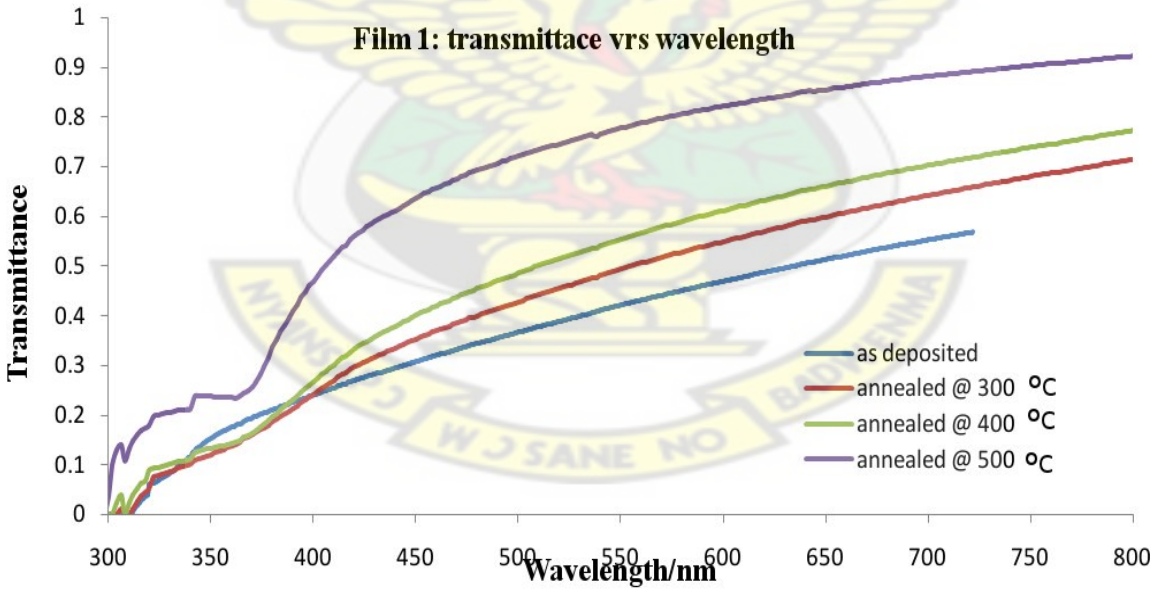

Figure 5.2A Optical transmission spectra variation of transmittance with annealing temperatures for Sample 1 with thickness 684 nm.

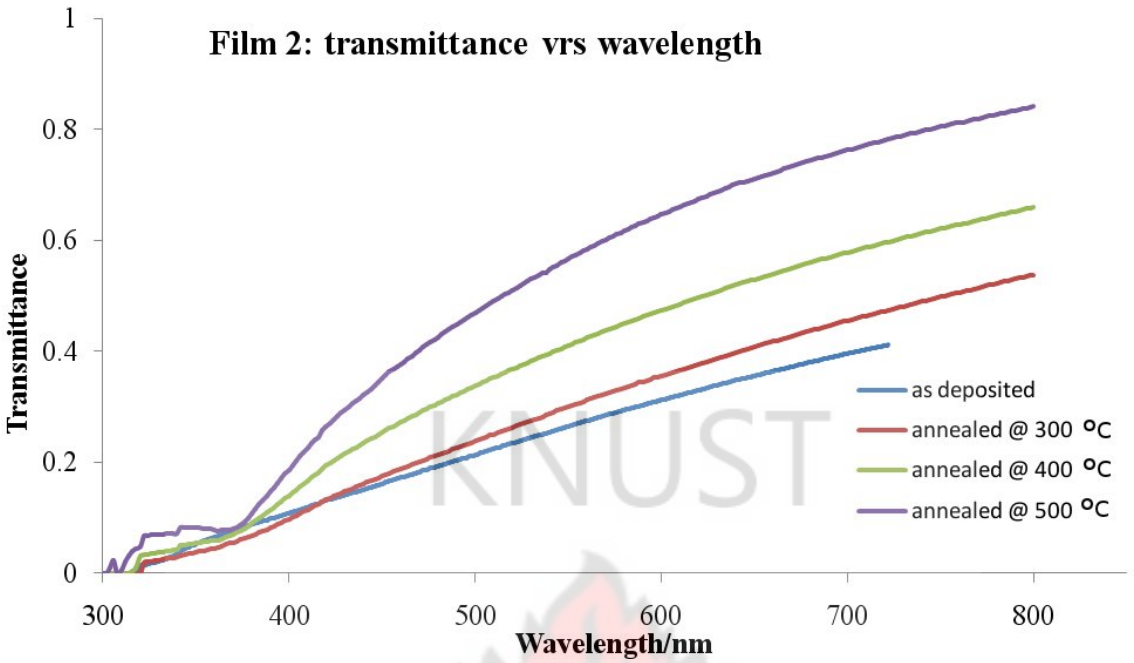

Figure 5.2B Optical transmission spectra variation of transmittance with annealing temperatures for Sample 2 with thickness 572 nm.

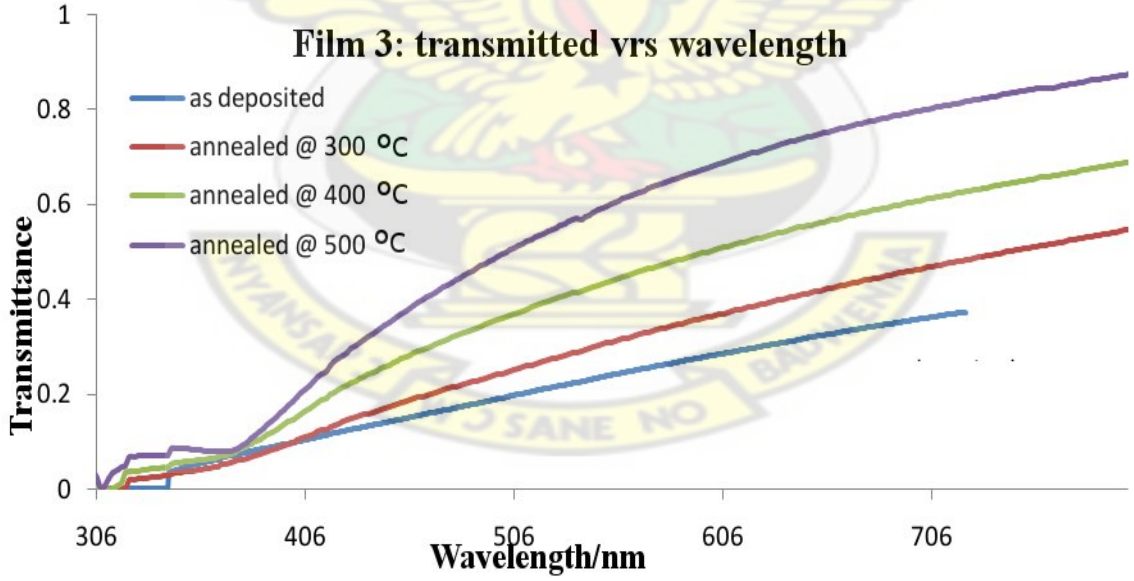

Figure 5.2C Optical transmission spectra variation of transmittance with annealing temperatures for Sample 3 with thickness 523 nm.

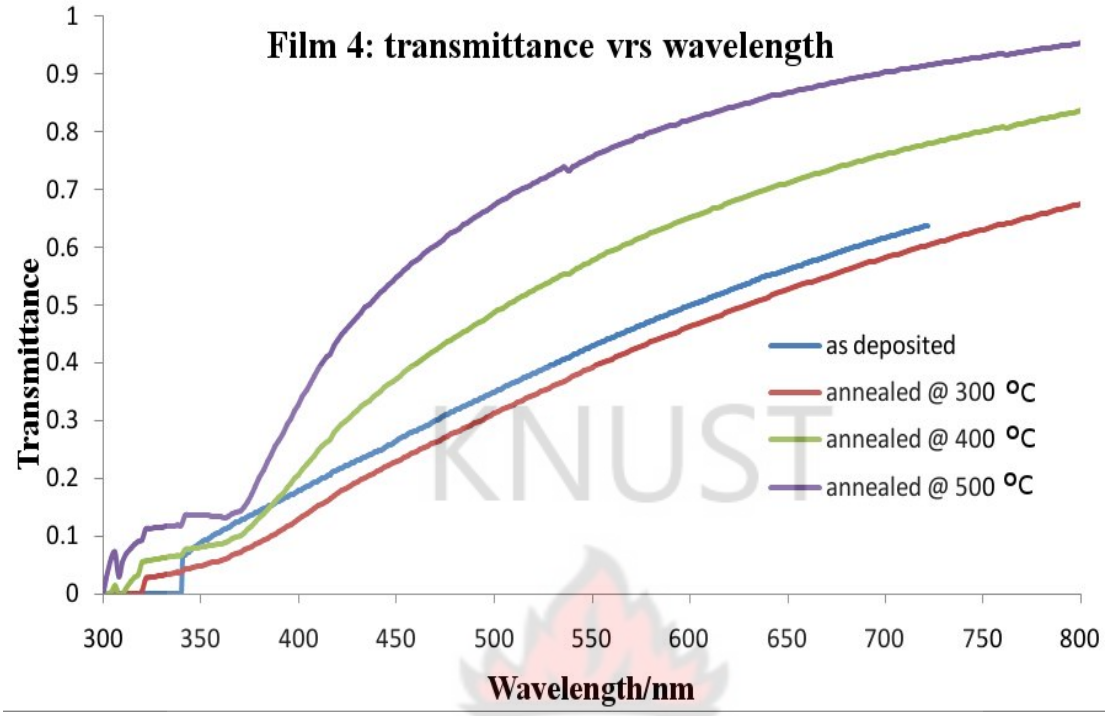

Figure 5.2D Optical transmission spectra variation of transmittance with annealing temperatures for sample 4 with thickness 271 nm.

An increase of the transmission values over the whole spectral range is observed with increasing annealing temperatures, especially within the visible region down to the near infra red (i.e 400-800 nm). For instance, at 700 nm, transmittance for Sample 1(with thickness of 684 nm) increased from 55 % through 64 %, 70 % to 80 % for as deposited, annealed at 300 ^{o}C, 400 ^{o}C and 500 ^{o}C respectively. Similar behavior was observed for all the other samples. This may be as a result of a decrease in grain size and or the decrease in the number of defects. Increase in transmittance with annealing temperature means that annealing produces better transmitter ZnS thin film semiconductor.

5.0.3 OPTICAL BAND GAP

The absorption coefficient, α, of the thin films is calculated from the absorbance spectrum by using the expression;

$$\alpha = \frac{1}{t}(2.303A) \qquad 1$$

Where A, is the absorbance, and d, is the thickness of the film.

Almost all the II-VI compounds are direct band gap semiconductors. The optical band gap of the thin films were estimated from absorption coefficient data as a function of wavelength by using the Tauc Relation for direct band gap materials, which is given by

$$\alpha h\upsilon = A(h\upsilon - E_g)^{1/2} \qquad 2$$

Where hυ, is the photon energy, E_g, the optical band gap and A is a constant.

By plotting a graph of $(\alpha h\upsilon)^2$ as ordinate and hυ as abscissa, the optical band gap E_g can be determined by the extrapolation of best fit line between $(\alpha h\upsilon)^2$ and hυ to intercept the hυ axis at $(\alpha h\upsilon)^2 = 0$. This intercept gives the value of the optical band gap of the material.

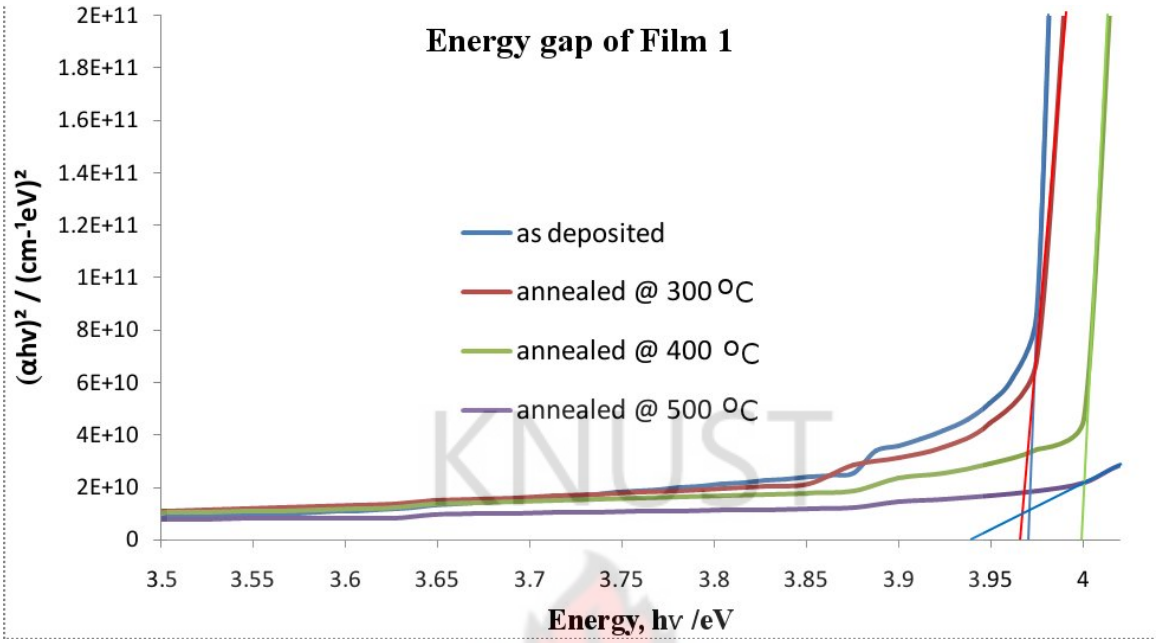

Figure 5.3A Plot of $(\alpha h\upsilon)^2$ versus photon energy, hυ showing variation of band gap with different annealing temperature for Sample 1 with thickness 684 nm.

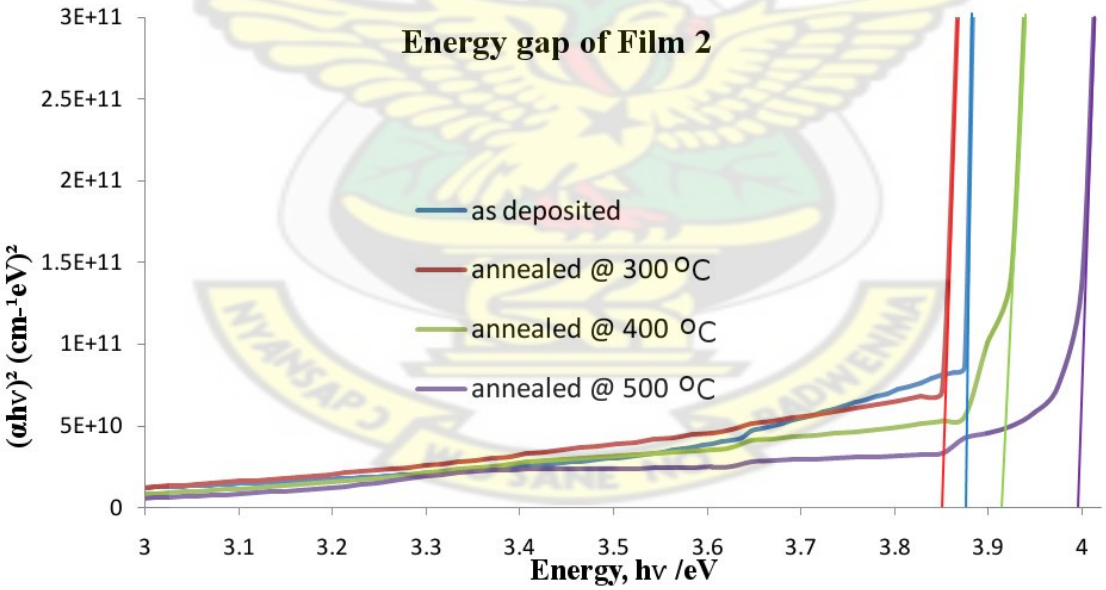

Figure 5.3B Plot of $(\alpha h\upsilon)^2$ versus photon energy, hυ showing variation of band gap with --- different annealing temperature for Sample 2 with thickness 572 nm.

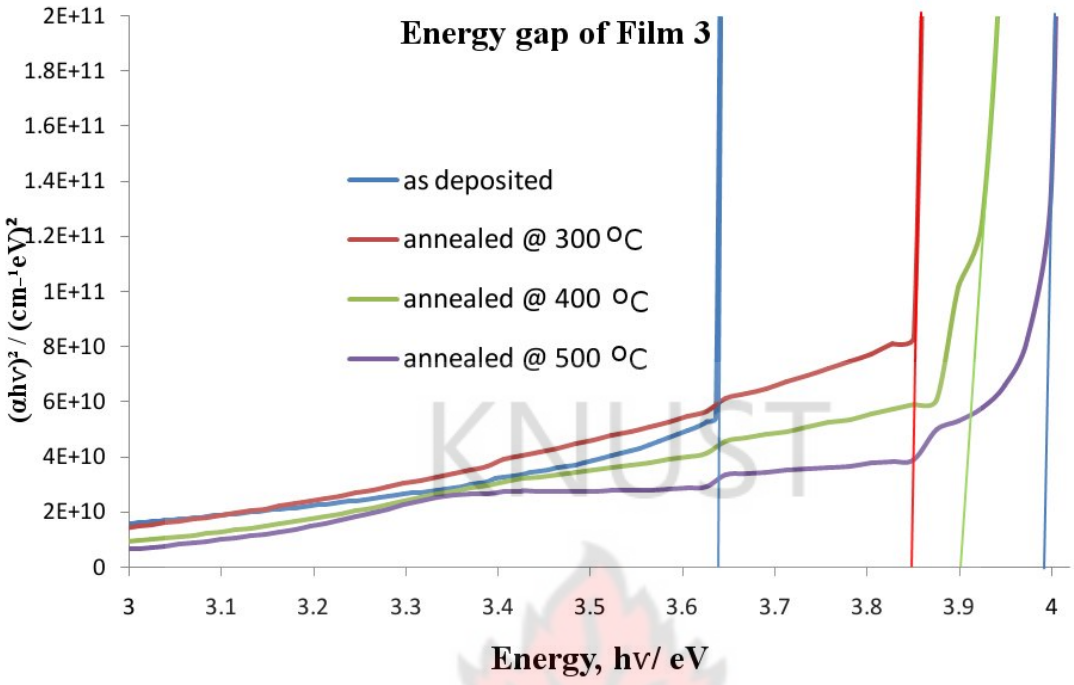

Figure 5.3C Plot of $(\alpha h\upsilon)^2$ versus photon energy, hυ showing variation of band gap with different annealing temperature for Sample 3 with thickness 523 nm.

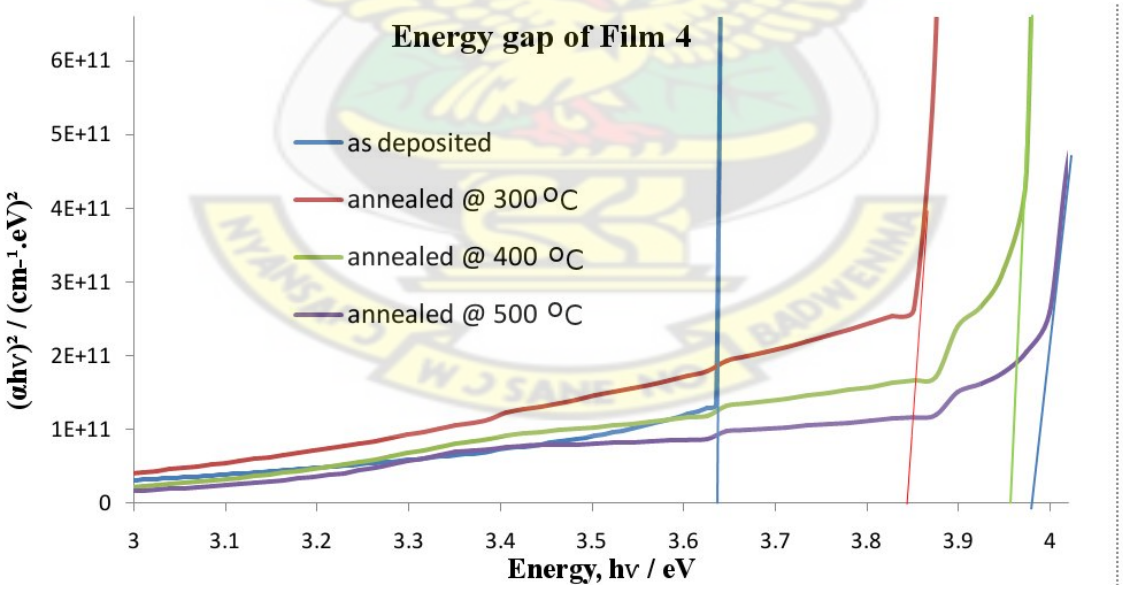

Figure 5.3D Plot of $(\alpha h\upsilon)^2$ versus photon energy, hυ showing variation of band gap with different annealing temperature for Sample 4 with thickness 270 nm.

From the figures the samples show an increase in the band gap with increasing annealing temperature. The temperature dependence parameters that affect the band gap are reorganization of the film, change in the crystallite size of the film and self-oxidation (Ezugwu *et al.*, 2009). During thermal annealing, the unsaturated defects are gradually annealed out (Hasegawa et al., 1978), producing large numbers of saturated bonds. The reduction in the number of unsaturated defects decreases the density of localized states in the band structure, and consequently increases the optical band gap (Dongol, 2002). Table 5.1 below is a summary of variation of band gap with annealing temperatures.

Table 5.1 Summary of variation of band gap with annealing temperatures for samples.

Sample	Thickness/ nm	Band gap (eV)			
		As deposited	Annealed @ 300^{o}C	Annealed @ 400^{o}C	Annealed @ 500^{o}C
1	684	3.97	3.97	4.00	3.94
2	572	3.88	3.85	3.92	4.00
3	523	3.64	3.85	3.90	3.99
4	271	3.64	3.84	3.91	3.98

5.0.4 EFFECT OF ANNEALING TEMPERATURES ON OPTICAL BAND GAP

It can be observed from Figure 5.4 that the film with thickness 684 nm shows no trend in band gap values with increasing annealing temperatures. However, the other three films (thicknesses: 572 nm, 523 nm, 271 nm) show general increase in band gap values with increasing annealing temperatures. As one anneals the films at these temperatures, various defects are reduced which decrease the density of localized states and improve

the crystallinity of the films.

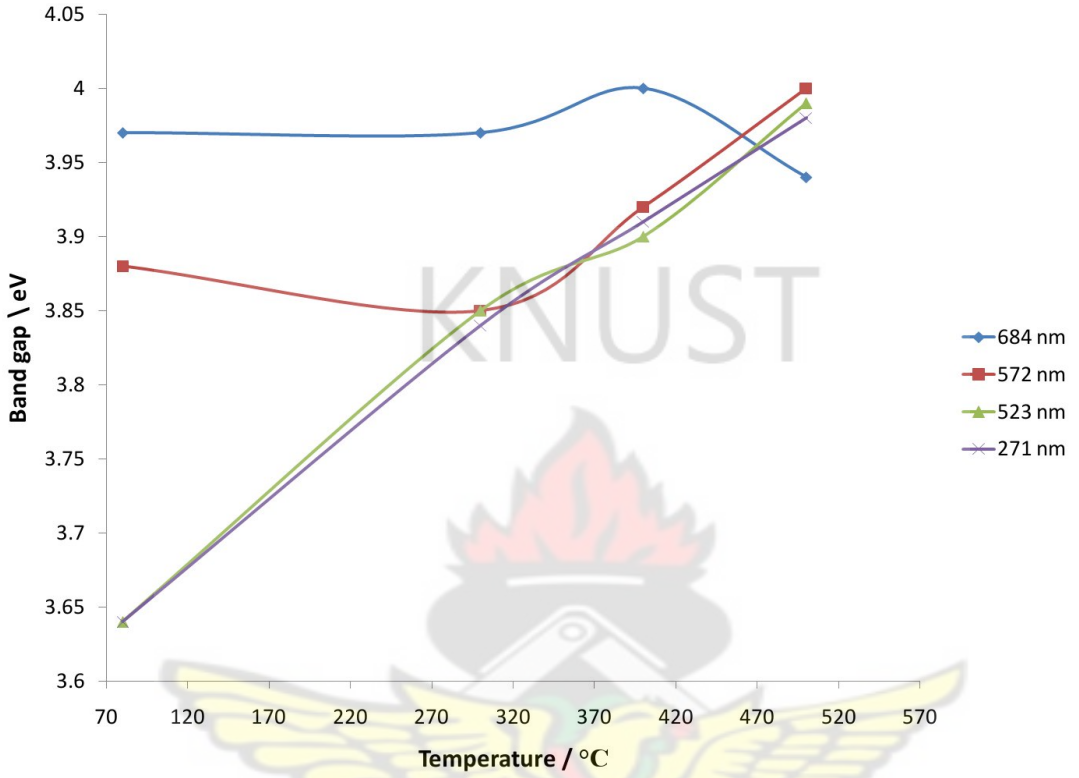

Figure 5.4 A plot of band gap values with increasing annealing temperatures for various film thicknesses.

5.0.5 MORPHOLOGY

The surface morphology of the as deposited films was assessed by scanning electron microscopy (SEM). Figure 5.4A shows a SEM micrograph of an as-deposited ZnS film. The films were dense and homogenous.

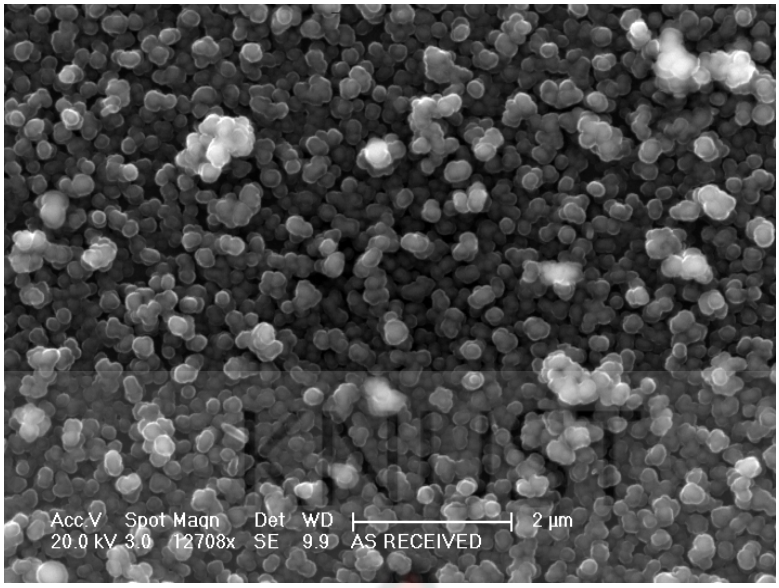

Figure 5.5A SEM micrograph of as-deposited ZnS thin films

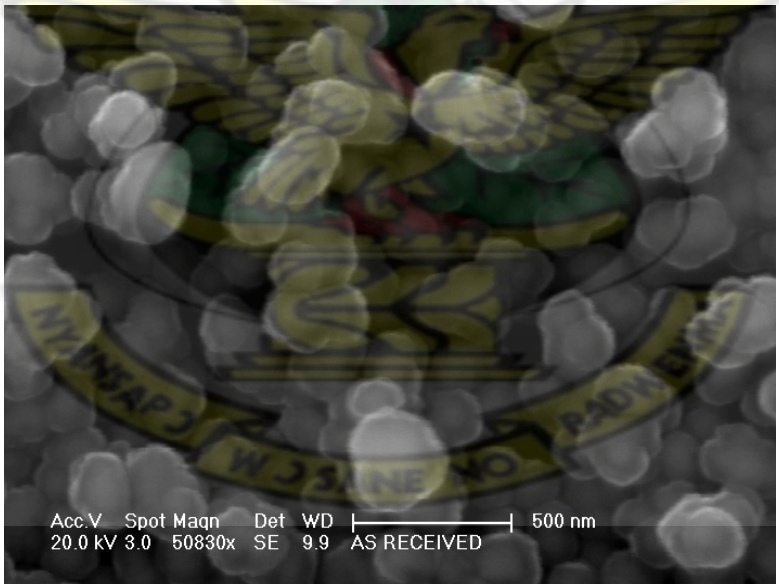

Figure 5.5B SEM micrograph of as-deposited ZnS thin films

Figure 5.5B shows an enlarged SEM micrograph of the as-deposited ZnS film shown in Figure 5.5A. The films appear to be dense and composed of largely irregular shaped

grains of diameter in the range of 300–500 nm. These large grains comprised smaller spherical grains of 10–200 nm diameter.

5.0.6 ENERGY DISPERSIVE ANALYTICAL X-RAY ANALYSIS (EDAX)

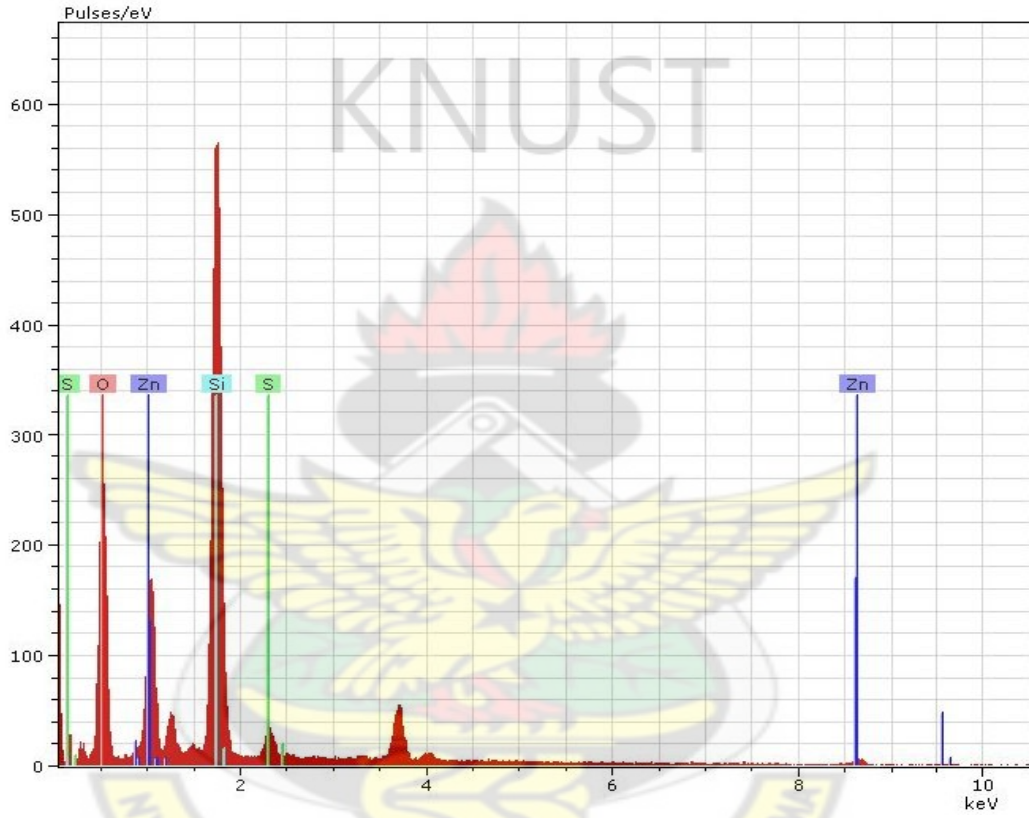

Figure 5.6A EDAX elemental analysis of as-deposited ZnS thin films

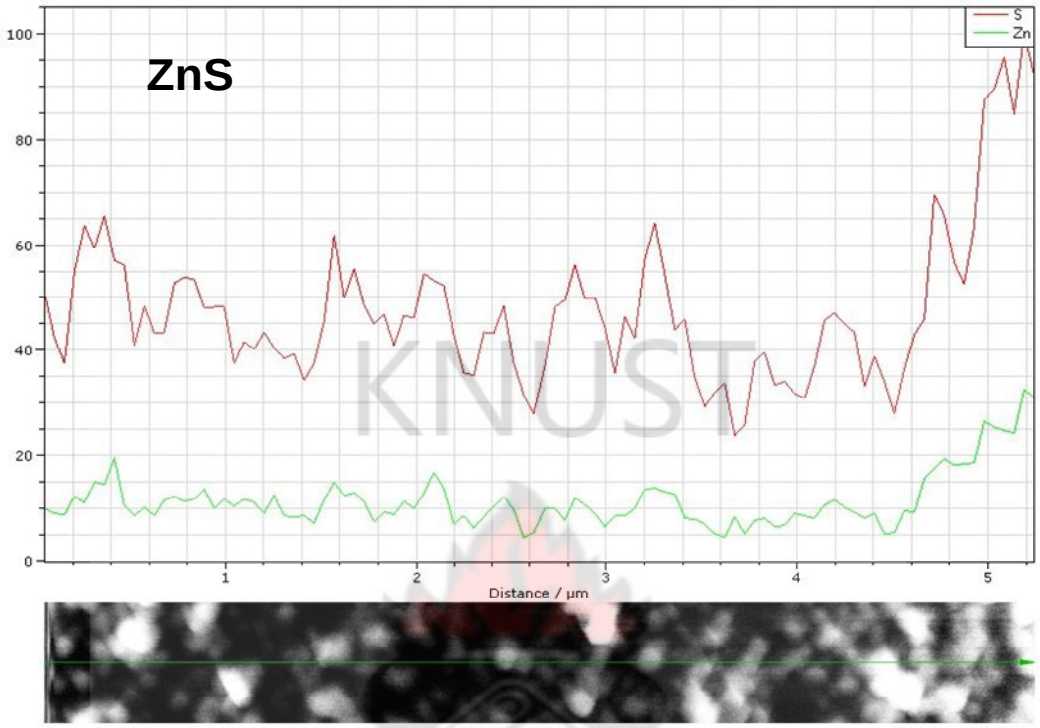

Figure 5.6B EDAX line scan of as-deposited ZnS thin films

Figure 5.6A and 5.6B show EDAX results which are consistent with the formation of thin films of ZnS deposited on silica glass substrates. It is widely known that CBD processes are associated with films which possess a relatively high concentration of impurities (ca. 0.1-1 % wt/wt) (Ortega-Borges et. al. 1993; Rieke at. al., 1993,). Table 5.2 shows the summary of the EDAX elemental analysis.

Table 5.2 Elemental analysis from EDAX results

Bruker AXS Microanalysis GmbH, Germany				18/02/2011
	Quantax			
Results				
Date: 18/02/2011				
Element	series	[wt.-%]	[norm. wt.-%]	[norm. at.-%]
Sulfur	K-series	1.4671956	1.61947685	1.157660739
Zinc	L-series	1.6880138	1.863213958	0.653134699
Calcium	K-series	16.678263	18.40931229	10.52889676
Magnesium	K-series	0.9866733	1.089080844	1.027107422
Sodium	K-series	5.6705107	6.259057141	6.24058971
Carbon	K-series	7.8623797	8.678421786	16.56200683
Aluminum	K-series	0.0321005	0.035432247	0.030101165
Silicon	K-series	36.870916	40.69777455	33.21542812
Oxygen	K-series	19.340832	21.34823033	30.58507455
	Sum:	90.596884	100	100

The presence of the large amount of impurities such as silicon, oxygen, magnesium, calcium and aluminum are suspected to be as a result of the microscope glass slide used as the substrate. These substances are the elemental composition of microscope glass slides, as given in appendix B.

5.0.7 X-RAY DIFFRACTION STUDIES

The amorphous nature of the thin film samples was confirmed by X-ray diffraction technique as no sharp peak was obtained, even after annealing at 400 ^{o}C as shown in Figure 5.7

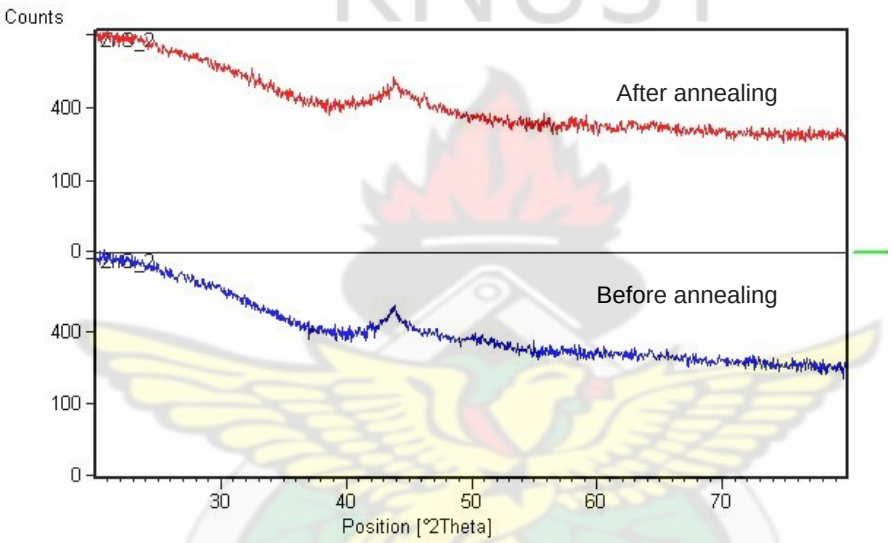

Figure 5.7 X-ray diffraction studies of the ZnS thin film

CHAPTER SIX

6.0 CONCLUSIONS AND RECOMMENDATIONS

6.1 CONCLUSIONS

A well adherent thin film of ZnS has been deposited on silica glass substrates from acidic baths containing zinc chloride, thioacetamide and urea. SEM micrograph of the as-deposited ZnS thin film, show the film to be uniform, dense, homogenous, and composed of largely irregular shaped grains of diameter in the range of 300–500 nm. These large grains comprised smaller spherical grains of 100–200 nm diameter. EDAX results are consistent with the formation of thin films of ZnS deposited on silica glass substrates. The optical absorbance of these films was measured by Schimadzu UV-VIS spectrophotometer within wavelength range of 200-800 nm. The films were annealed at temperatures of, 300 ^{o}C, 400 ^{o}C and 500 ^{o}C for one hour. It was observed that the absorbance decreased whereas transmittance increased with increasing annealing temperature. This may be as a result of improvement in the crystalline state of the sample. The optical band gap of the films was also determined from the absorption spectra. The optical band gaps of the films before and after annealing were between 3.64-4.00 eV. These values compare well with values obtained by other researchers, shown in appendix A.

6.2 RECOMMENDATIONS

- Electron Diffraction measurements to ascertain whether the samples are amorphous or polycrystaline.

- Hall Effect measurements should be carried out to determine the conductivity type.

REFERENCE

Antony, A., Murali K. V., Manoj R., Jayaraj M. K., (2005). Quoted by Eid A. H., Salim S. M., Sedik M. B., Omar H., Dahy T., Abou_elkhair H. M., (2010). Preparation and Characterization of ZnS Thin Films. *Journal of Applied Sciences Research*, 6(6): 777-784.

Al Kuhaimi, S.A. and Tulbah, Z., (2000). *J. Electrochem. Soc*., **147**, 214

Anderson, F. (1959), Acta Chem Scond 8 pp. 1599. Cited by Madon A. and Shaw M. P., (1988). The Physics and Application of Amorphous Semiconductors. *Academic Press Inc. London*

Beal, S. E., (1978). Cleaning and Surface Preparation, *Thin Solid Films*, **53**, 97.

Blos, W.H.N., Pfisterer , F., Shock, H.W., (1998). Quoted by Boyle, D.S., Robbe, O., Hallida, D.P., Heinrich, M.R., Bayer, A. ,O'Brien, Otway, D.J. and Potter, M.D.G., (2000). *Journal of Material Communication Chemistry*.

Chopra, K.L., (1969). Thin Film Deposition Technology, *McGraw Hill*; New York, pp. 55-68.

Chopra K. L., Kainthla R. C., Pandra D. K. and Takoor A. P., (1982). *Phys. Thin Films*, 12, 167.

Chopra, K.I. and Kaur. I., (1983). Thin Film Device Applications. Plenum, New York

Davis E. A. and Mott N. F. (1970). Quoted by M. Dongol (2002). Optical Absorption and Structural Properties of as-deposited and Thermally Annealed As-Te-Ga Thin Films *Egypt. J. Sol*., 25, (1), 33.

DonÄa J. M. and Herrero J., (1995). Quoted by David S. Boyle, Odile Robbe, Douglas P. Halliday, Markus R. Heinrich, Alexander Bayer, Paul O'Brien, David J. Otwaya and Mark D. G. Potter., (200). *Journal of Materials Communication Chemistry.* 10, 2439-2441

Dongol M., (2002). Optical Absorption and Structural Properties of as-deposited and Thermally Annealed As-Te-Ga Thin Films *Egypt. J. Sol*., 25, (1), 33

Edelson, V (2007). *Concentration Crisis.* In Brown Alumni Magazine, July/August 2007

Electronics (2010) Encyclopedia Britannica. *Encyclopedia Britannica Deluxe Edition*. Chicago: Encyclopedia Britannica.

Ezugwu S. C., Ezema F. I., Osuji R. U., Asogwa P. U., Ezekoye B. A., Ekwealor A. B. Chigbo C., Anusuya M., and Mahaboob Beevi M., (2009). Quoted by Asogwa P. U., (2011). Band Gap Shift and Optical Characterization of Pva-Capped PbO Thin Films: Effect Of Thermal Annealing. *Chalcogenide Letters,* 8, (3), pp.163 – 170

Gellings, P.J. and Bouwmeester, H. J. M., (1997). The CRC Handbook of Solid State Electrochemistry, *CRC Press*, p.84.

Göde F., Gümüş C., Zor M., (2007). Investigations on the Physical Properties of the Polycrystalline ZnS Thin Films Deposited by the Chemical Bath Deposition method. *Journal of Crystal Growth.* Volume 299, (1), pp 13-14

Gilbert B., Frazer B. H., Zhang H., Huang F., Banfield J. F., Haskel D., Lang J. C., Srajer G., De Stasio G. (2002). Quoted by Nasra B. T., Kamouna N., Kanzari M.,

Bennaceur R., (2006). Effect of pH on the properties of ZnS thin films grown by chemical bath deposition. *Journal of Thin Solid Films,* 500, pp 4 – 8

Greenwood N. and Earnshaw A., (1984). *Chemistry of the Elements*, Oxford: Pergamon, p. 1405, ISBN 0-08-022057-6

Gomezdaza A., Sanchez O., A., Campos J., Hu H., Suarez R., Rincón M. F., (1998) Sol. Energy *Mat. Sol. Cells,* 52, 313.

Gonellien, J. (1996) Quoted by Nadeem, M.Y., Ahmed, W., Wasiq M.F., (2005, Sct). ZnS Thin Films – An Overview . *J of Research (science) ; Buhauddin Zakaniya University, Multan, Pakistan*-Vol.16, pp105.H.D, (1995) J. Opt. soc. Amer.42,21

Hammer K., (1943). *Z. Techn. Phys.,* 24, 169p

Hasse, M.A., Qui, J., DePuydt, J.M., Cheng, H., (1991). *Appl. Phys. Lett*., 59, 1272.

Hasegawa S., Yazalci S. and Shimizu T., (1978). Quoted by M. Dongol (2002). Optical Absorption and Structural Properties of as-deposited and Thermally Annealed As-Te-Ga Thin Films *Egypt. J. Sol*., Vol. (25), No. (1), 33.

Hodes, G., (2002). Chemical Solution Deposition of Semiconductor Films. New York, pp.3-6.

Huldt and Staflin, Gonellian. Cited in Nadeem, M.Y., Ahmed, W., Wasiq M.F., (2005). ZnS Thin Films – An Overview . *J of Research (science) ; Buhauddin Zakaniya University, Multan, Pakistan*-Vol.16, pp105.

Ilenikhena P. A., (2008). Comparitive Studies of Improved Chemical Bath Deposited Copper Sulphide (CuS) and Zinc Sulphide (ZnS) Thin Films at 320K and Possible Applications. *Journal of African Physical Review*, **2**: 0007 59

Johnston D. A., Carletto M. H., Reddy K. T. R, Forbes I. and Miles R., (2002). W. *Thin Solid Films.* 403-404 102-6

Kashani H., (1996). *Thin solid Films*, 288(1-2).

Kassim, A., Nagalingam, .S.,Tee T.W., sharif, A.M., Abdulah, D. K., Elos M. J and Min, H.S., (2009). Effect Deposition Period and PH on Chemical Deposition Cuns4 thin Films, *Philipians Journal of science* 138(2): 161-168.

Kittel, C., (2005). Introduction to Solid State Physics, Eighth Edition. *John Wiley & Sons, Inc*. p.577

Korvink, J.G. and Greiner, A., (2002). Semiconductors for micro- and Nanotechnology an Introduction for engineers, p.40.

Katsumi K., (1995). Jpn. *J.Appl. Physics*, pp 33,4383.

Li, S.S., (2006). Semiconductor Physical Electronics, Second Edition, pp.246-253, p.335.

Lindroos, S., Kannianen, Tapio., Leskela,M.(1997) Quoted by Nadeem, M.Y., Ahmed, W., Wasiq M.F., (2005). ZnS Thin Films – An Overview . *J of Research (science) ; Buhauddin Zakaniya University, Multan, Pakistan*-Vol.16, pp105.

Mattox, D. M., (1978). Surface Cleaning in Thin Film Technology, *Thin Solid Films*, No. 1, **53**, 81.

Nadeem M.Y., Ahmed W., Wasiq M.F., (2005). ZnS Thin Films – An Overview . *J of Research (science) ; Buhauddin Zakaniya University, Multan, Pakista*n-Vol.16, pp105.

Nadeem, .M.Y., Ahmed,W.(2000), Turk. *J.Phys*., 24651

Nair P. K., Nair M. T. S., Garcıa V. M., Arenas O. L., Pena Y., Castillo A., Yala I. T.

Ndukwe, I.C (1996) *Solar Energy Materials and Solar Cells* , 40,123.

Nadeem, M.Y., Ahmed, W., Wasiq, M.F., (2005). ZnS Thin Films – An Overview . *J of Research (science) ; Buhauddin Zakaniya University, Multan, Pakista*n-Vol.16, pp105.

Neamen, D.A., (2003). Semiconductor Physics and Devices, Basic Principles, Third Edition, p.2, pp. 144-145.

O'Brien P. and McAleese J., (1998). Quoted by Jie Cheng, DongBo Fan, Hao Wang, BingWei Liu, YongCai Zhang and Hui Yan. Chemical bath deposition of crystalline ZnS thin films. *Journal of Semicond. Sci. Technol.* 18 No 7 (July 2003) 676-679 PII: S0268-1242(03)58148-2

O'Brien, P. and J. McAleese, (1998), Quoted by Vaughn Edelson (2007). Concentration Crisis. *In Brown Alumni Magazine,* July/August 2007.

Ohring, M., (1992). The Materials Science of Thin Films, *Academic Press*, San Diego. pp. 195-199, 336-339.

Ortega, R., Borges, D. (1992). *Lincot and Vedel, in Proc. 11th ed. E.C Photovoltaic solar Energy Conf* **.,** Hawood Academic Publishers, Switzerland,p862.

Padam G. K., Rao S. U. M. and Maholtra G. L. (1988), *J. Appl. Phys*., 63, 770

Petterson, J. D. and Bailey, B. C., (2005). Solid-State Physics Introduction to the Theory, pp.293-294, 113, 637.

Pillai S.O., (2009). *Solid state Physics. India*: New Age Int. (P) Ltd. Publishers, pp 523, 539-540, 696-697, 700, 704.

Polster, H.D (1952). J. Opt. soc. Amer. 42, 42

Poole, C.P.Jr., (2004). Encyclopedic Dictionary of Condensed Matter Physics, vol.1 p. 66, 440, 1391.

Rood, J.L. (1951). Quoted by Nadeem, M.Y., Ahmed, W., Wasiq M.F., (2005, Sct). ZnS Thin Films – An Overview. *J of Research (science) ; Buhauddin Zakaniya University, Multan, Pakistan*-Vol.16, pp105.H.D, (1995) J. Opt. soc. Amer.42,21.

Savadogo O. (1998). Sol. Energy Mat. Sol. Cells 52, 361

Singh, J., (2003). Electronic and Optoelectronic Properties of Semiconductor Structures, *Cambridge University Press*; New York, p. IV, 51-52.

Singh, J., (2006). Optical Properties of Condensed Matter and Applications, *John Wiley and Sons, Ltd*. pp.2-4.

Sole, J. G., Bausa, L. E. and Jaque, D., (2005). An Introduction to the Optical Spectroscopy of Inorganic Solids, pp. 11-12.

Tan W.C. (2006). *Optical properties of amorphous selenium films* Thesis University of Saskatchewan, pp. 3-13

Tauc, J., (1974). Amorphous and Liquid Semiconductors, Plenum: New York, p. 159.

Thwilis J (1979) Quoted by Nadeem, .M.Y, Ahmed, W., Wasiq M.F., (2005, Oct). ZnS Thin Films – An Overview . J of Research (science) ; *Buhauddin Zakaniya University, Multan, Pakistan*-Vol.16, pp105.

Ubale, A.U. and D.K. Kulkarni, 2005. Quoted by A.H. Eid, S.M. Salim, M.B. Sedik, H. Omar, T. Dahy, H.M. Abou_elkhair (2010). Preparation and Characterization of ZnS Thin Films. *Journal of Applied Sciences Research*, 6(6): 777-784, 2010 © 2010, INSInet Publication

Venables, J.A., (2003). Introduction to Surface and Thin Film Processes, *Cambridge University Press*. Cambridge. pp 5--60.

Vipin, K., Sharma, M.K., Gaur, J., Sharma, T.P., (2008). Polycrystalline Zns Thin Films By screen Printing Method And Its Characterization, *J chalcogenide Letters Vol.5, No 11:p 289, 291*.

Wasiq M.F., (2005). ZnS Thin Films – An Overview . *J of Research (science ; Buhauddin Zakaniya University, multan, Pakistan*, 16, pp105.

Wells, A. F. (1984), *Structural Inorganic Chemistry* (5th ed.), Oxford: Clarendon Press, ISBN 0-19-855370-6

Yacobi, B. G., (2004). Semiconductor Materials: An Introduction to Basic Principles, pp.1-3, 154-157, 107.

Yamaga S., Yoshokawa A. and Kasain H.,(1998). Cited in K. R. Murali, and S. Kumaresan. (2009). Characteristics of Brush Plated ZnS Films *Chalcogenide Letters* Vol. 6, (1), pp. 17 –22

Yamaguchi, T., Yamamoto, Y., Tanaka, T., Demizu, Y. and Yoshida, A., (1996). *Thin Solid Films*, **281/282**, 375.

Young, H.D. and Freedman, R.A., (2008). *University Physics with Modern Physics*, 12th Edition, pp. 1449-1455.

Zainal Z., Zobir Hussein M., Ghazali A., (1996). Solar Energy Materials and Solar Cells, **40**, 347

Zendehnam A., Shirazi M., Doulatshah S., and Sadat M., (2010). Effect Of Temperature And Period Of Post-Annealing On The Optical Properties Of ZnO Thin Films. *Armenian Journal of Physics,* vol. 3, (4), pp. 305-311

APPENDIX A

Table A.1: Comparison of Optical Band Gap energy of ZnS Thin Films

Scientists	Methods	Optical Band gap (eV)
Lindroos *et al.* (1997)	SILAR	3.44
Nomura *et al.* (1995)	MOVPE	3.50
Yamaguchi *et al*. (1996)	CBD	3.60
Biswas *et al.* (1986)	CBD	3.68
Ndukwe (1996)	CBD	~3.7 – 3.8
Nadeem and Ahmed (2000)	R – H	3.51 – 3.84
Gode et al, (2007)	CBD	3.79 – 3.93
Ubale et al, (2007)	CBD	3.68 – 4.10

APPENDIX B

Table B.1: HDA Microscope slides are manufactured from normal glass or super white glass. Chemical Composition of normal glass:

Silicon Dioxide	SiO_2	72.00%
Sodium Oxide	Na_2O	14.50%
Potassium Oxide	K_2O	0.30%
Calcium Oxide	CaO	7.05%
Magnesium Oxide	MgO	3.95%
Aluminium Oxide	AL_2O_3	1.65%
Ferric Oxide	Fe_2O_3	0.06%
Density : 2.50 x 10^3 kg/m^3		

Courtesy of Yancheng huida medical instruments co.,Ltd (Tel: +86-515-88387981 88389440 Fax: +86-515-88387982 E-mail: info@huidamedical.com.cn)